Optimization of Subsite Binding to the β5 Subunit of the Human 20S Proteasome Using Vinyl Sulfones and 2-Keto-1,3,4-oxadiazoles: Syntheses and Cellular Properties of Potent, Selective Proteasome Inhibitors

Robert M. Rydzewski,*,† Leland Burrill,† Rohan Mendonca,† James T. Palmer,† Mark Rice,† Ram Tahilramani,† Kathryn E. Bass,‡ Ling Leung,‡ Erik Gjerstad,§ James W. Janc,§ and Lin Pan||

Departments of Medicinal Chemistry, Cell Biology, Enzymology, and Distribution, Metabolism, and Pharmacokinetics, Celera Genomics, 180 Kimball Way, South San Francisco, California 94080

Received December 27, 2005

Beginning with the peptide sequence Cbz-Ile-Glu(O*t*Bu)-Ala-Leu found in PSI (**3**), a series of vinyl sulfones (VS) were synthesized for evaluation as inhibitors of the chymotrypsin-like activity of the 20S proteasome. Variations at the key P3 position confirmed the importance of a long side chain capped with a hydrophobic group for optimal potency, consistent with a model of binding to the S3 subsite. The *tert*-butyl glutamic ester initially used at P3 gave plasma unstable, insoluble compounds and was replaced with the better isostere, *N*-β-neopentyl asparagine. The inhibitors were shortened by replacing the *N*-terminal Cbz-isoleucine with a *p*-tosyl group without loss of potency. Small L-amino acids were used at P2, where D-substitution was not tolerated. The resulting optimized P4-P3-P2 sequence was grafted onto a novel proteasome inhibitor warhead, 2-keto-1,3,4-oxadiazoles (KOD), to produce reversible, subnanomolar proteasome inhibitors that were 1000-fold selective versus cathepsin B (CatB), cathepsin S (CatS), and trypsin-like as well as PGPH-like proteasome activity. A number of compounds in both the VS and the KOD series exhibited growth inhibitory effects against the human prostate cancer cell line PC3 at submicromolar concentrations.

Introduction

Controlled proteolysis of cellular proteins is a process vital to cell survival, proliferation, and even death. Improperly folded or damaged proteins as well as many intact ones, such as cyclins, cyclin dependent kinase inhibitors, and MHC class I antigens, do not generally suffer the fate of either uncatalyzed hydrolysis or degradation by lysosomal enzymes but instead are destroyed via the ubiquitin-proteasome pathway.[1] Conjugation with ubiquitin, a 76-amino acid protein generally attached through a lysine side chain of the target protein, begins the ATP-driven process, which is consummated within the inner chamber of the 26S proteasome where twin sets of three different catalytically active subunits carry out the proteolysis.[2] The large, barrel-shaped core of the 26S proteasome, which lacks the 19S regulatory subunits but is otherwise enzymatically competent, is known as the 20S proteasome or core particle (CP). Elegant work using scanning electron microscopy,[3] X-ray crystallography,[4] and mutation analysis[5] has elucidated structural and functional aspects of the proteasome. The three catalytic subunits, known as β1, β2, and β5 utilize *N*-terminal threonine residues to cleave peptides having basic, acidic, and hydrophobic residues in their P1 positions, respectively.[4a]

Interest in interfering with this biologically important process stems from the potential for therapeutic utility. The proteasome degrades IκBα, an endogenous inhibitor of nuclear translocation for the important protein NF-κB, which has antiapoptotic as well as many other cellular effects.[6] In addition, the proteasome is required for the production of the p50 subunit of NF-κB. Inhibiting the proteasome, which is also responsible for the destruction of tumor suppressor protein p53 and may regulate the concentrations of a number of proteins controlling cell cycle progression,[7] should therefore increase the levels of apoptosis, thereby exerting anticancer effects. Theory has yielded to current clinical practice through the approval of the proteasome inhibitor bortezomib (**1**), shown in Figure 1, which has demonstrated statistically significant beneficial effects and is currently used to treat patients with multiple myeloma.[8]

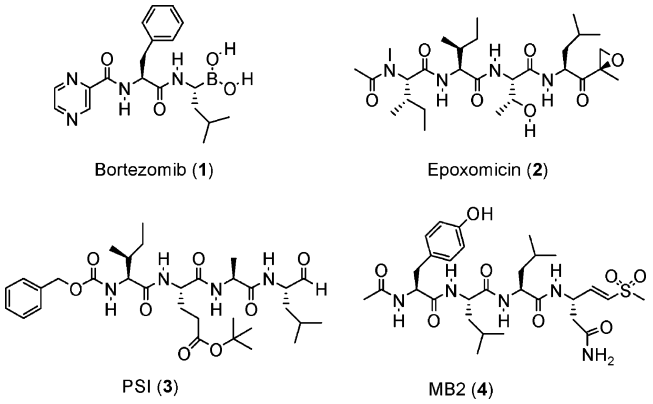

Figure 1. Structures of Bortezomib, Epoxomicin, PSI, and MB2.

The proteasome has also been proposed to play a role in HIV infectivity,[9] and several teams report that a number of HIV protease inhibitors are also weak proteasome inhibitors.[10] Other therapeutic areas where inhibiting the proteasome could have a therapeutic effect include inflammatory[11] and cerebrovascular[12] diseases. Clearly, there is a need for novel, small molecule proteasome inhibitors to be used as tool compounds in exploring the many cellular pathways involving this unique and ubiquitous enzyme.

Figure 1 presents a number of known small molecule inhibitors of the 20S proteasome. To date, only a limited number of

* To whom correspondence should be addressed. Tel: 510 795-8711. E-mail: brydzewski@sbcglobal.net.
† Department of Medicinal Chemistry.
‡ Department of Cell Biology.
§ Department of Enzymology.
|| Department of Distribution, Metabolism, and Pharmacokinetics.

10.1021/jm058289o CCC: $33.50
Published on Web 04/21/2006

Scheme 1[a]

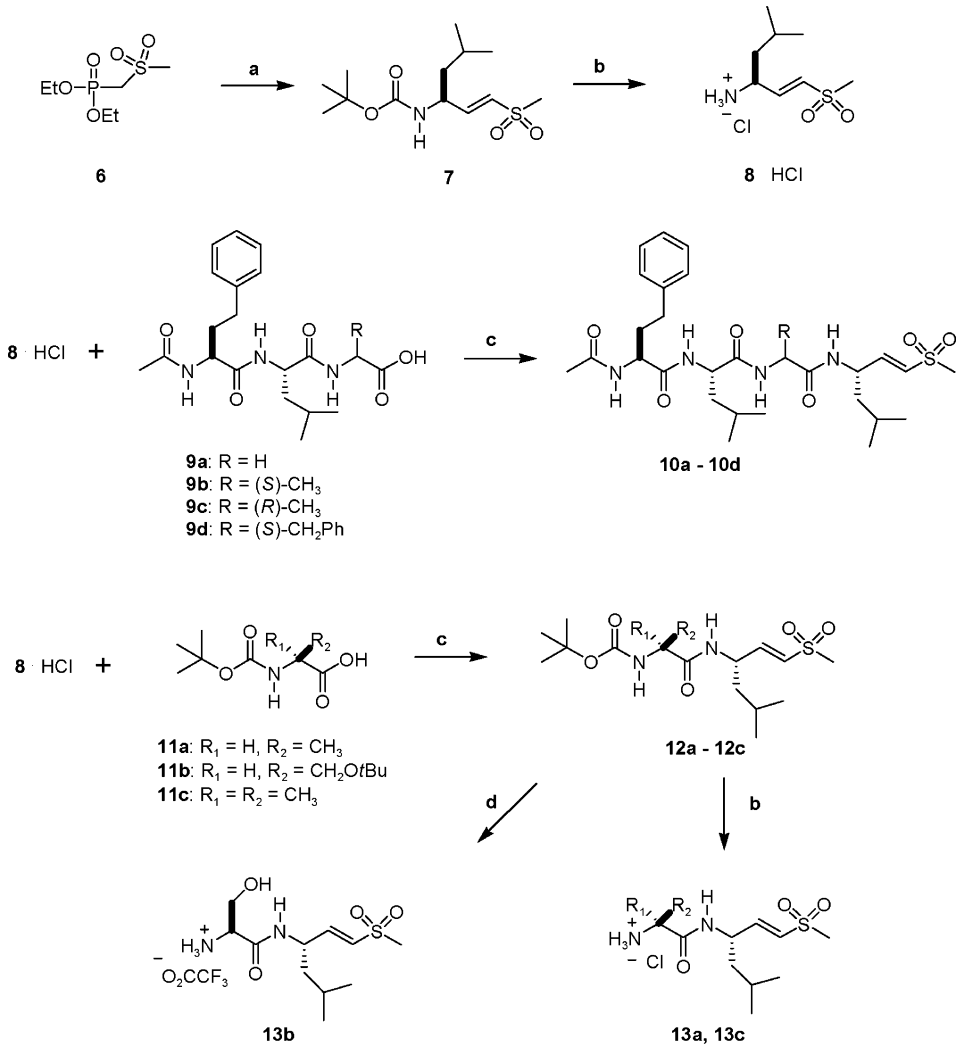

[a] Reagents: (a) NaH, Boc-Leu-H, THF, 0 °C; (b) HCl/dioxane; (c) IBCF, NMM, THF, −10 °C; (d) TFA.

SAR studies aimed at optimizing substituents at various positions have been reported for proteasome inhibitors. Bogyo[13] used scanning libraries to develop a β2 specific inhibitor. Positional scanning libraries have also been used to study substrate interactions at β1,[14] whereas Crews[15,16] has reported epoxomicin analogues with β1 and β5 selectivity. SAR optimization, selectivity data versus various antitargets, and profiles of cellular properties are all vitally needed to evaluate compounds for in vitro and in vivo use. We herein report the syntheses, activities, selectivities, and selected properties for two different series of 20S proteasome inhibitors, the irreversible series of vinyl sulfones (VS)[17] **10a**−**d**, **17a**−**t**, and **22a**−**o** as well as the novel, reversible 2-keto-1,3,4-oxadiazoles (KOD) **29a**−**l**.

Chemistry

Vinyl sulfone **8**, shown in Scheme 1, has been previously reported.[18] This compound was prepared by the Horner−Emmons reaction of Boc leucinal with sulfone **6**[19] followed by deprotection with HCl. Compounds **10a**−**d** were prepared by mixed anhydride coupling of vinyl sulfone **8** with capped tripeptides **9a**−**d**, which had been made by standard solid-phase syntheses on Wang resin. In an analogous fashion, mixed anhydride coupling of **8** with a Boc-protected amino acid (**11a** and **c**) and subsequent deprotection using HCl gave dipeptide analogues **13a** and **c**. In the case of P2 serine, side chain protection via *tert*-butyl ether (**11b**) was used, and the subsequent treatment of **12b** with TFA in place of HCl afforded the bis-deprotected product **13b**.

Compounds **17a**−**t** (Scheme 2) in the long, tetrapeptide-like vinyl sulfone series were prepared by one of two routes. Either tripeptide **16** was coupled with P1 amine **8** (Method A) or Cbz dipeptide **14** was coupled with dipeptide amines **13a**−**c** (Method B). Negligible racemization (<5%) was encountered in the final coupling by either method, so long as mixed anhydride coupling was carried out below 0 °C. Requisite dipeptides **14a**−**t** were either commercially available (**14a**, **14b**, **14t**), synthesized by standard Fmoc chemistry on Wang resin (**14c**−**f**, **14i**, **14l**, **14m**), or prepared by solution phase coupling of the free P3 amino acid with the succinate ester of Cbz isoleucine (**14g**, **14h**, **14j, 14k, 14n**−**s**). In Method A, dipeptides **14** were converted to the corresponding succinate esters **15** by reaction with NHS in the presence of DCC, whereas in Method B, the free acid was used in the subsequent coupling reaction.

As shown in Scheme 3, where side chain amide derivatives of aspartic or glutamic acid were required (**14o**−**s**), the starting monomers were prepared by EDC/HOAt coupling of the desired side chain amine with the corresponding α-*N*-Boc protected amino *tert*-butyl ester followed by global deprotection. The experimental procedure for the preparation of **14q** is an example of this route. Scheme 3 also shows the synthetic route used to

Scheme 2[a]

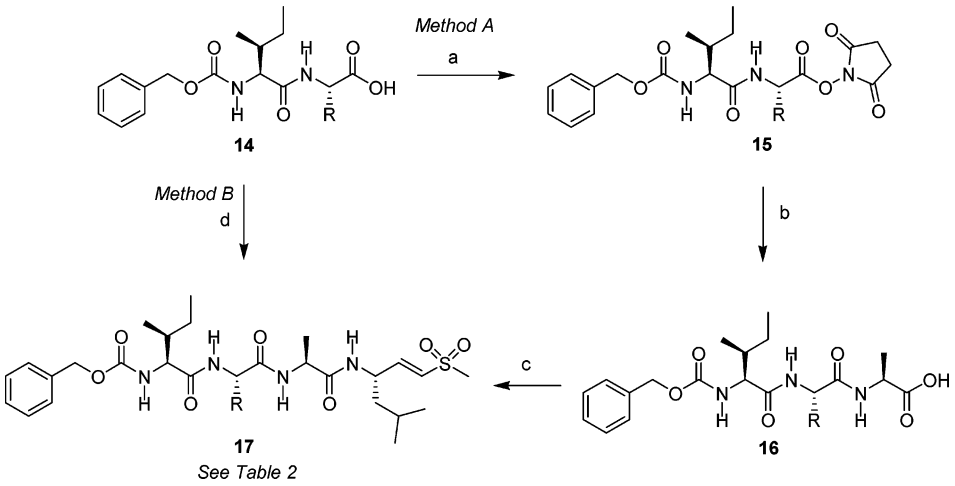

[a] Reagents: (a) *N*-Hydroxysuccinimide, DCC, THF; (b) L-alanine, Et_3N, aq THF; (c) **8**, IBCF, NMM, THF, −10 °C; (d) **13**, IBCF, NMM, THF, −10 °C.

Scheme 3[a]

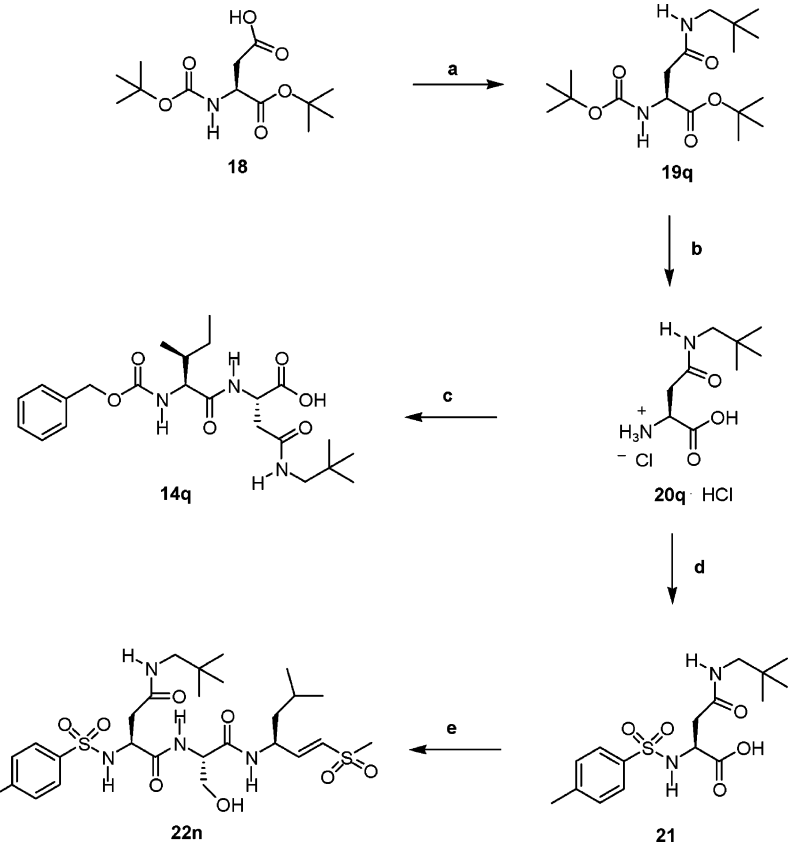

[a] Reagents: (a) Neopentylamine, EDC, HOAt, DMF; (b) HCl/dioxane; (c) Cbz-Ile-OSu, Et_3N, aq THF; (d) *p*-Tosyl chloride, NaOH, aq dioxane; (e) **13b**, IBCF, NMM, THF, −10 °C.

prepare tripeptide vinyl sulfones **22a**−**o**. The desired *N*-terminal group was attached to the P3 amino acid under Schotten−Baumann conditions, and the resulting adduct was coupled to dipeptide vinyl sulfone **13** via the mixed anhydride.

The KODs **29a**−**l** were synthesized according to the route shown in Scheme 4. Oxadiazole **23** was lithiated, then transmetalated at low temperature as previously reported by Nakai.[20] The resulting magnesio species reacted with Boc leucinal to give **24** as a mixture of diastereomers. Deprotection gave **25**, which could be coupled to the P2 Boc amino acids to afford **26**. Another deprotection followed by coupling to the desired N-functionalized P3 acid gave **28**. The N-functionalized P3 acids were, in turn, synthesized by reaction of the corresponding P3 amino acid with the appropriate sulfonyl chloride under Schotten−Baumann conditions. For the P3-substituted benzyl compounds **28i**−**l**, the requisite amino acids were prepared by direct alkylation of Boc serine using two equiv of NaH and one equiv of the substituted benzyl bromide in DMF. Oxidation of diastereomeric mixture **28** using the Dess−Martin periodinane afforded **29** in good yield.

The α-heteroaryl carbonyl groups of compounds **29a**−**l** were sufficiently electrophilic that small amounts (∼5%) of hydrates $(m + 18)^+$ were observed as peaks separate from the main product in the LCMS spectra, except in the case of the hindered

Scheme 4[a]

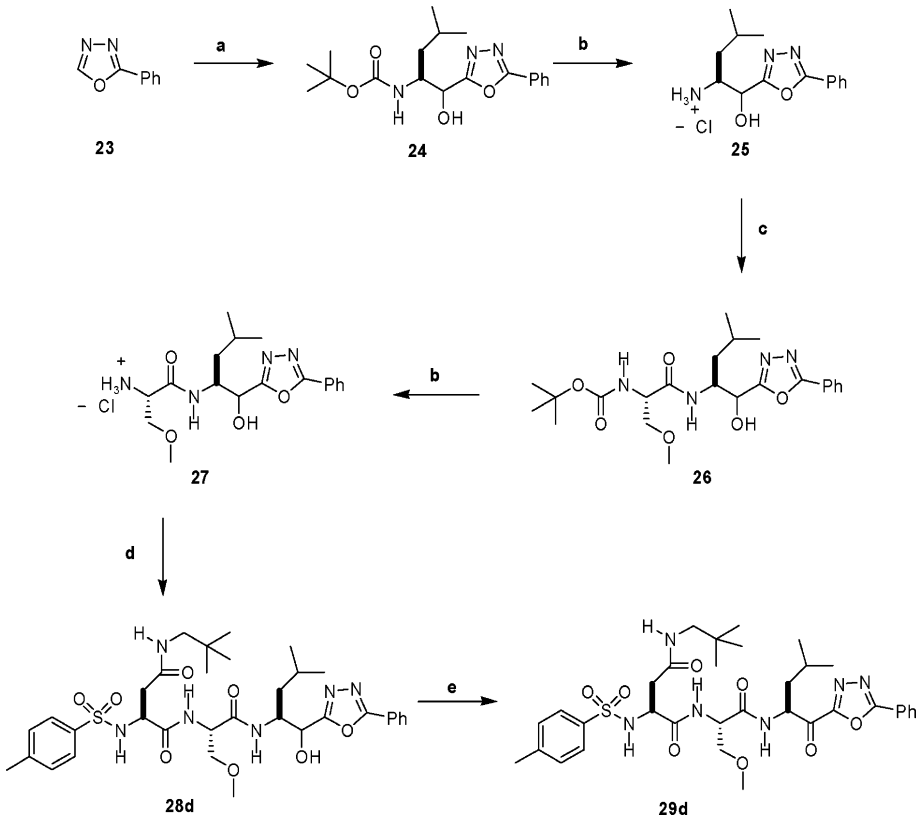

[a] Reagents: (a) *i*. *n*-BuLi, THF, −78 °C, *ii*. $MgBr_2 \cdot Et_2O$, −78 °C, *iii*. Boc-Leu-H, −78 °C; (b) HCl/dioxane; (c) Boc-Ser(OMe)-OH, EDC/HOBT, NMM, CH_2Cl_2; (d) **21**, EDC/HOBT, NMM, CH_2Cl_2; (e) Dess−Martin periodinane, wet CH_2Cl_2.

Table 1. Inhibition Constants for Some Proteasome Inhibitors

compd	value[a]	ChT-L[b]	Tryp-L[c]	PGPH[d]	CatB[e]	CatS[f]
2	IC_{50}	0.0037	0.16	2.2	120	25
3	Ki_{app}	<0.001	2.7	14	nd[g]	nd
5a	Ki_{app}	0.0023	110	48	nd	nd
5b	Ki_{app}	0.0037	0.33	.47	0.012	nd
5c	Ki_{app}	>450	nd	nd	18	0.046
10a	IC_{50}	1.3	nd	nd	>150	12
10b	IC_{50}	0.12	nd	nd	1.6	6.9
10c	IC_{50}	56	nd	nd	>150	77
10d	IC_{50}	0.035	>150	>150	0.85	0.15

[a] The type of inhibition constant. [b] The value (μM) for chymotrypsin-like proteasome activity. [c] The value (μM) for trypsin-like proteasome activity. [d] The value (μM) for post glutamyl peptide hydrolase-like proteasome activity. [e] The value (μM) for cathepsin B activity. [f] The value (μM) for cathepsin S activity. [g] Not determined.

P1 Aib[17] analogue, **29e**. The samples of **29a**−**d** and **29f**−**l** that had been dissolved in methanol for LCMS analysis also tended to show the reversibly formed methyl hemiketal, $(m + 32)^+$, as another separate peak that was more prominent than the hydrate, but this adduct was entirely absent when ACN was used as the solvent. In all cases, however, NMR spectra in DMSO-d_6 showed the desired product present as a single species characterized by the downfield-shifted P1 methine proton around δ 5.1.

Results and Discussion

The search for novel proteasome inhibitors suitable for testing in cellular and in vivo models began with a determination of the enzymatic activities for the known proteasome inhibitors shown in Table 1. The inhibition constants shown in Table 1 are of two different types. The values for irreversible inhibitors, where inhibition is by definition a nonequilibrium, time-dependent process,[21] are shown as IC_{50} values after a 1 h inhibitor/proteasome incubation, whereas Ki_{app} values are used to characterize reversible inhibitors. This allows for SAR comparisons within a given series and selectivities versus antitargets for a given compound to be derived, but values of different types should not be directly compared. Inhibition constants were obtained for chymotrypsin-like, trypsin-like, and PGPH-like proteasome activities of the human 20S proteasome. These reflect proteolysis at the active sites of the β5, β2, and β1 subunits, respectively.[22] Experiments using mutations in active site subunits of the yeast proteasome demonstrated that of the three activities, chymotrypsin-like activity was the one most necessary for cell viability and protein processing,[23] and existing proteasome inhibitors target this β5 activity.

In general, subsite selectivity was not a significant issue for any of the inhibitors, with the exceptions of epoxide **2** and aldehyde **5b**, where only moderate selectivities versus trypsin-like and PGPH-like activities were observed. This lack of cross-reactivity could be rationalized in terms of the varying P1 and P3 steric and electronic requirements for the different subunits. Selectivity versus cysteinyl cathepsins, the major sources of lysosomal proteolysis in cells, was potentially a bigger problem. Previously described warheads for proteasome inhibitors, including vinyl sulfones[24] and aldehydes[25], are known to also target enzymes such as cathepsin B (CatB) and cathepsin S (CatS), where the active site sulfhydryl group of the cysteine protease can form a covalent bond to the electrophile when the inhibitor is appropriately substituted. For example, peptidyl vinyl sulfones, originally reported as inhibitors of cathepsins,[24] were later reported by Bogyo et al[18] to be active proteasome inhibitors when properly extended. Assays for the inhibition of CatB and CatS, performed as previously described,[26] revealed that several of the compounds in Table 1, including the aldehyde MG-132

Table 2. SAR of Tetrapeptide Vinyl Sulfones

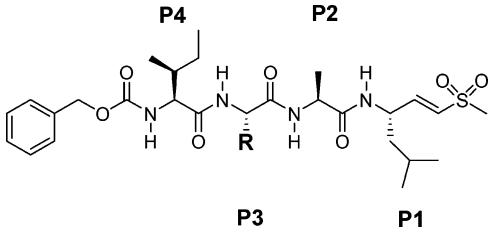

compd	method	R	ChT-L[a]	Tryp-L[b]	PGPH[c]	CatB[d]	CatS[e]
17a	A	$CH_2CH(CH_3)_2$	0.069	39	>150	5.8	0.7
17b	A	CH_2Ph	0.46	nd[f]	nd	27	9
17c	A	CH_2CH_2Ph	0.027	>150	>150	41	10
17d	A	(*E*)-CH_2CH═$CHPh$	0.044	nd	nd	nd	nd
17e	A	CH_2OCH_2Ph	0.049	>150	>150	38	35
17f	A	$CH_2SO_2CH_3$	3.3	nd	nd	140	13
17g	A	$CH_2SO_2CH_2Ph$	1.4	nd	nd	>150	12
17h	B	CH_2CO_2(*t*-Bu)	0.078	>150	>150	nd	nd
17i	A	$CH_2CO_2CH_2Ph$	2.5	nd	nd	nd	nd
17j	A	$CH_2CH_2CO_2$*t*-Bu	0.0025	>150	>150	29	36
17k	B	$CH_2CH_2CH_2CO_2$(*t*-Bu)	0.024	>150	>150	18	7.1
17l	A	$CH_2CH_2CO_2(C_6H_{11})$	0.01	nd	nd	nd	nd
17m	A	$CH_2CH_2CONH_2$	0.57	nd	nd	54	48
17n	B	$CH_2CH_2CH_2CONH_2$	0.12	nd	nd	nd	nd
17o	B	CH_2CH_2CONH(*i*-Pr)	0.052	>150	>150	>150	41
17p	B	CH_2CH_2CONH(*t*-Bu)	0.0032	>150	>150	51	3.3
17q	B	$CH_2CONHCH_2C(CH_3)_3$	0.0015	>150	>150	nd	nd
17r	B	$CH_2CH_2CONHCH_2C(CH_3)_3$	0.049	>150	>150	nd	nd
17s	B	$CH_2CH_2CONHC(CH_3)_2CH_2CH_3$	0.0024	>150	>150	nd	nd
17t	B	see Figure 2	150	nd	nd	23	13

[a] IC_{50} (μM) for chymotrypsin-like proteasome activity. [b] IC_{50} (μM) for trypsin-like proteasome activity. [c] IC_{50} (μM) for post glutamyl peptide hydrolase-like proteasome activity. [d] IC_{50} (μM) for cathepsin B activity. [e] IC_{50} (μM) for cathepsin S activity. [f] Not determined.

(**5b**), are submicromolar cathepsin inhibitors. The corresponding peptide nitrile **5c**[27] was devoid of proteasome activity, possibly indicating the failure of the enzyme's active site to accommodate the resulting sp^2 (versus sp^3 for other electrophiles) intermediate. Nitrile **5c**, however, was a 46 nM inhibitor of CatS, emphasizing the importance of electrophile selection to inhibitor selectivity.

Having observed good proteasome inhibition with the P1 keto epoxide, aldehyde, and boronate but not the nitrile electrophiles, we decided to produce a focused series of peptidyl vinyl sulfones, where the effects of substitution at P2 could be assessed. The P5-P4-P3-P2 sequence used in the case of **10d**, Ac-hPhe-Leu-Phe, stems from an optimized proteasome inhibitor in the keto epoxide series reported by Crews.[15] Although vinyl sulfone **10d** was the most potent of the four P2 analogues against chymotrypsin-like proteasome activity (35 nM), it also displayed 150 nM potency as a CatS inhibitor. The removal of its P2 phenyl ring in the Ala analogue **10b** resulted in a 3-fold loss of proteasome activity. The replacement of L-Ala with D-Ala at P2, potentially of interest to discourage unwanted in vivo proteolysis, gave 56 μM **10c**. The observed 500-fold diminution of activity in reversing the stereochemistry of the methyl group at P2 was not easily explained on the basis of sterics but may reflect a shift in the conformational space away from the bound conformation for this ligand. The P2 Gly analogue **10a** was about 10-fold less potent than the L-Ala, emphasizing, along with the 1600-fold difference in activities between the most- and least-potent members of this small series, that specific binding requirements at P2 cannot be disregarded in proteasome inhibitor design.

One of the promising, potent, and selective proteasome inhibitors shown in Table 1 is PSI (**3**), an inhibitor first reported by Wilk.[28] Although the potential for metabolism, Schiff base formation, and, perhaps, nonspecific inhibition may be sufficiently troubling to rule out optimization of aldehydes as a viable route to improved proteasome inhibitors, the peptide sequence of **3** seemed to be a good starting point for optimization studies using a different P1 electrophile. For reasons previously noted, Ala was retained at P2, whereas its P3 *tert*-butyl glutamic ester, an unusual structural feature and one suspected to be key to good binding at S3, was replaced with a number of analogues in a series featuring the robust, readily accessible vinyl sulfone electrophile. Table 2 summarizes the resulting SAR.

Compound **17j**, the vinyl sulfone analogue of **3**, proved to be a 2.5 nM inhibitor of chymotrypsin-like proteasome activity. Selectivities versus trypsin-like and PGPH-like proteasome activities as well as CatB and CatS, were at least 10 000-fold, and in general, the selectivities tended to be high for all of the compounds in the series. The replacement of the *tert*-butyl glutamic ester with smaller residues such as Leu **17a** (69 nM) or Phe **17b** (460 nM) resulted in diminished activity. Although larger P3 replacements tended to fare well, attesting to the preference for large hydrophobic interactions at S3, hydrophobicity was optimally placed at the distal end of the side chain; simple, extended linear chains such as Gln (**17m**, 570 nM) and hGln[17] (**17n**, 120 nM) were not potent. The trend thus observed is consistent with modeling predictions. As shown in Figure 3, the interface between the β5 and β6 subunits, which constitutes the S3 binding cleft, can accommodate long, linear side chains, but the best opportunity for hydrophobic interactions lies at the end of the resulting cleft. That the *tert*-butyl Glu ester fits this well is attested to by observing that both the shorter *tert*-butyl Asp ester (**17h**, 78 nM) and the longer *tert*-butyl hGlu[17] ester (**17k**, 24 nM) are an order of magnitude less active. Unfavorable interactions along the linear part of the binding cleft may account for the micromolar potencies encountered with sulfonyl-containing analogues **17f** and **g**. The replacement of the *tert*-butyl Glu

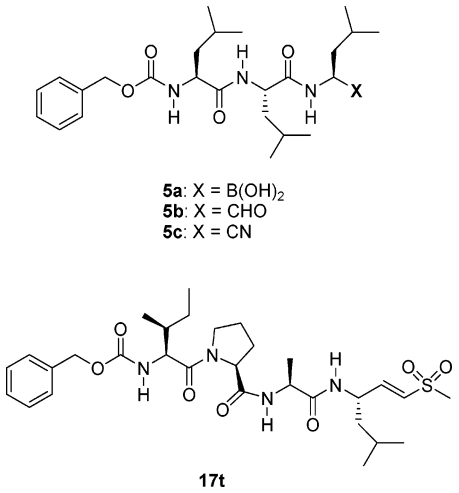

Figure 2.

ester with the cyclohexyl Glu ester gave another potent compound, **17l** (10 nM).

Uncertainty about whether such *tert*-butyl esters would be substrates for esterase-catalyzed in vivo hydrolysis provided the impetus for the synthesis of several isosteres. The amide isostere of **17j**, *tert*-butyl Gln **17p** (3.2 nM), was about equipotent to the ester but was presumably more difficult to hydrolyze. The importance of a single methyl group in hydrophobic S3 interactions was emphasized by the nearly 20-fold loss of activity observed with corresponding *i*-propyl Gln amide **17o** (52 nM). Another advantageous isostere, the neopentyl Asn amide **17q** proved to be the most potent compound in the series at 1.5 nM, and therefore, this *tert*-butyl Glu ester analogue was used extensively in subsequent inhibitors.

Although the potencies and selectivities of these compounds were favorable, considering the size and relatively high molecular weights of these molecules led us to suspect that other properties such as solubility and cell permeability might not be favorable. Our molecular weight loss program began with an exploration of substituent requirements at P4 and P5. Table 3 summarizes the results for this series, where the Cbz-Ile *N*-terminus of compound **17** was replaced with a simple capping group on the *N*-terminus of the P3 residue. Although the replacement of the *N*-terminus of **17j** with a simple acetyl group (**22a**) resulted in a 100-fold loss of potency, most of this activity was restored upon replacement with an phenyl-containing substituent such as the benzoyl group (**22b**, 17 nM), the Cbz group (**22c**, 6.1 nM), or, better still, the *p*-tosyl group (**22g**, 2.1 nM), which was equipotent with **17j** but nearly 100-fold lower in molecular weight. As predicted, and as shown in Table 5, the kinetic solubility of **22g**, at 48 μM, was greater than that of **17j** ($<$10 μM). Despite concerns stemming from a report that P4 modifications in a series of vinyl sulfone proteasome inhibitors can affect subunit selectivity,[29] all P4 analogues shown in Table 3, which were tested against the trypsin-like and PGPH-like activities of the proteasome, were found to be inactive.

Combining the newly found P4 *p*-tosyl group with the neopentyl Asn P3 isostere gave **22m**, a 4.3 nM proteasome inhibitor with good (470 μM) solubility. The replacement of the P2 Ala with Ser, which was expected to improve solubility still further, gave **22n**, a 5.9 nM inhibitor with slightly reduced (361 μM) solubility relative to the Ala analogue **22m**. Other modifications in this shortened vinyl sulfone series including using BocDab[17] as a P3 isostere (**22i**), placing still more hydrophobicity at the distal end of the P3 substituent (**22k**, **22l**), and attempting to prophylactically block potential in vivo proteolysis with the P2 Aib group (**22o**) resulted in losses in potency of several orders of magnitude.

Having simplified the original Cbz-Ile-Glu(O*t*Bu)-Ala sequence of **3** to the smaller, more soluble, and presumably more stable *p*Ts-NeopentylAsn-Ala sequence of VS **22m**, we decided to incorporate this sequence into a new series of reversible proteasome inhibitors. A number of known drugs, including aspirin and penicillin, are irreversible enzyme inhibitors,[21,30] and at least a few irreversible inhibitors including a rhinovirus 3C protease inhibitor[31] are reported to be in development. One might also debate the physiological consequences of using an irreversible inhibitor versus a reversible, slow off-rate (or functionally irreversible) inhibitor.[32] Still, widespread concern about potential nonspecific inhibition and immunogenicity suggest that reversibility be preferred for pharmacological intervention. A series of P1 modifications led to the discovery that the 2-keto-1,3,4-oxadiazole (KOD) warhead previously known to be active in inhibitors of neutrophil elastase[20] and HepC NS3 protease[33] could also function as a potent electrophile for the proteasome β5 subunit active site.

The reversibility of the inhibition of chymotrypsin-like 20S proteasome activity was established for KOD **29c** through experiments in which the 20S proteasome was incubated with the inhibitor at a concentration that fully inhibited enzyme activity. After incubation, the enzyme−inhibitor complex was diluted 50-fold into a substrate-containing buffer. The chymotrypsin-like activity of the proteasome, initially fully inhibited, slowly recovered with a first-order rate constant of 0.010 min^{-1} ($t_{1/2}$ = 68 min). The final steady-state enzyme activity was 65% of the control reaction in which the 20S proteasome was not exposed to the inhibitor. This value is consistent with the establishment of a new equilibrium after the dilution of the inhibitor and enzyme by 50-fold. These results fit with a model of reversible inhibition with slow decomposition of the tetrahedral hemiketal intermediate at the active site.

Table 4 shows the structures and activities of the KODs. Grafting the preferred sequence found in VS **22m** onto the LeuKOD P1 moiety gave **29c**, a 720 pM inhibitor of chymotrypsin-like 20S proteasome activity, which was $>$50 000-fold selective against antitargets. As in the VS series, compounds lacking a phenyl ring at P4, such as **29a** and **29f**, tended to be less active. Substituting the *meta*-tosyl for the *para*-tosyl group gave the essentially equipotent compound **29b** (650 pM). The PBS solubility of **29d** (37 μM), a P2 methyl Ser compound, was slightly improved relative to that of the corresponding Ala compound **29c** (13 μM), whereas the potency remained the same. The solubility was not increased by the substitution of a *p*-dimethylamino group on the phenyl ring of the ketooxadiazole (**29g**, $<$10 μM), but potency may have improved slightly (510 pM versus 720 pM), suggesting that further prime side modifications might prove fruitful. Substituting Aib[17] for Leu at P1 resulted in a 180-fold loss of potency (**29e**), as might have been expected in light of the known affinity of the enzyme subunit for moderately sized, hydrophobic side chains in substrates at this position.[34]

A different P3 unit was also pursued in a series of several analogues. The P3 benzyl Ser residue found in **17e**, a VS, gave reasonable inhibition at 49 nM, although about 30-fold less potent than the corresponding neopentyl Asn (**17q**). Compounds **29i**−**l** were synthesized to test whether this was transferable to the KOD series and, if so, whether potency could by optimized by substituents on the phenyl ring. At 32 nM, the proteasome

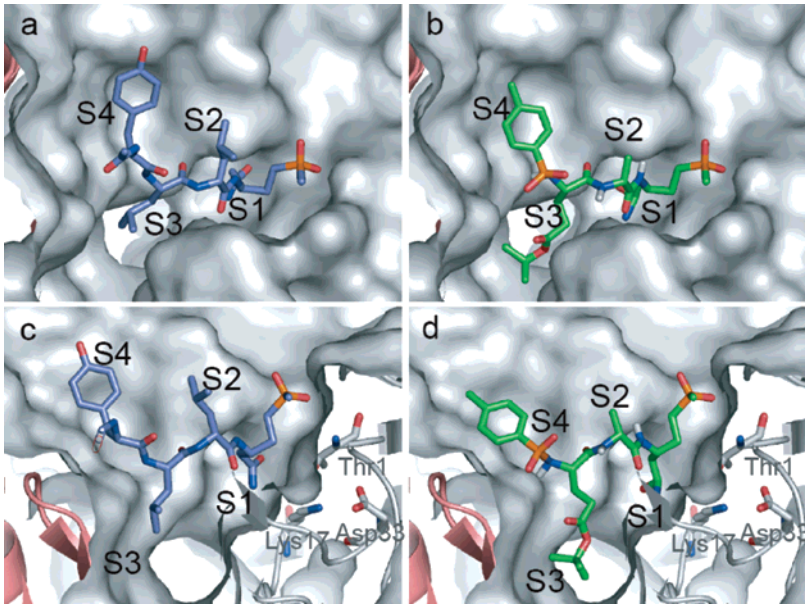

Figure 3. (a) **MB2** top view, (b) **22g** top view, (c) **MB2** side view, and (d) **22g** side view. The catalytic residues are shown as stick figures in c and d. All inhibitors are docked into the β5 (grey) and β6 (pink) subunits of the bovine proteasome structure 1IRU using the MMF94 force field in MOE (Chemical Computing Group, Montreal, Quebec) as rendered in Pymol (DeLano Scientific, South San Francisco, CA).

Table 3. SAR of Tripeptide Vinyl Sulfones

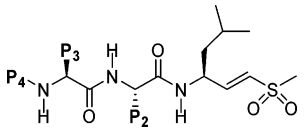

compd	P4	P3	P2	ChT-L[a]	Tryp-L[b]	PGPH[c]	CatB[d]	CatS[e]
22a	acetyl	*t*-butylGlu	Ala	0.26	nd[f]	nd	77	170
22b	benzoyl	*t*-butylGlu	Ala	0.017	>450	>450	nd	nd
22c	Cbz	*t*-butylGlu	Ala	0.0061	>150	>150	20	3
22d	Cbz	*t*-butylGlu	Gly	0.17	nd	nd	>150	21
22e	Cbz	*t*-butylGlu	Ser	0.0029	>450	>450	nd	nd
22f	$PhSO_2$	*t*-butylGlu	Ser	0.0011	>450	>450	nd	nd
22g	*p*-tosyl	*t*-butylGlu	Ala	0.0021	>450	>450	13	67
22h	Ph_2CHCO	*t*-butylGlu	Ala	0.0067	>450	>450	nd	nd
22i	Cbz	BocDab[17]	Ser	0.43	nd	nd	nd	nd
22j	acetyl	benzylGlu	Ala	21	nd	nd	nd	nd
22k	Cbz	CH_2CONH-(*S*)-$CH(t\text{-bu})CO_2t$-bu	Ala	0.54	nd	nd	nd	nd
22l	Cbz	$CH_2CH_2CONHC(CH_3)_2CO_2t$-bu	Ala	2.3	nd	nd	nd	nd
22m	*p*-tosyl	neopentylAsn	Ala	0.0043	>450	>450	nd	nd
22n	*p*-tosyl	neopentylAsn	Ser	0.0059	>450	>450	>150	>150
22o	*p*-tosyl	neopentylAsn	Aib[17]	28	>450	>450	nd	nd

[a] IC_{50} (μM) for chymotrypsin-like proteasome activity. [b] IC_{50} (μM) for trypsin-like proteasome activity. [c] IC_{50} (μM) for post glutamyl peptide hydrolase-like proteasome activity. [d] IC_{50} (μM) for cathepsin B activity. [e] IC_{50} (μM) for cathepsin S activity. [f] Not determined.

inhibition observed for parent compound **29i** was about 40-fold less than that of matching neopentyl Asn **29d**. Unfortunately, small substituents in the ortho (**29j**, 45 nM), meta (**29k**, 140 nM), and para (**29l**, 500 nM) positions only served to decrease potency in this series. Figure 4 models the binding of **29c**, a P3 neopentyl Asn compound and the corresponding *o*-tolyl Ser compound **29j** in the active site of the β5 subunit, and shows one of the *tert*-butyl methyl groups reaching down into a part of the S3 pocket that may not be accessible to phenyl substituents in the benzyl Ser analogues.

At this point, potent and selective proteasome inhibitors had been made in both the VS and the KOD series. These compounds were investigated as potential tool compounds for purposes of cellular and animal testing. Beyond simple in vitro potency and selectivity, other parameters must be met for such compounds to be useful in biological systems. Kinetic solubility in PBS can be measured to provide insight into the less easily quantified but the more important property of formulability. Because the proteasome is found in cytosol, cell permeability can be assessed to see whether the inhibitors can reach the target. Finally, because metabolism can occur in plasma, principally by the action of nonspecific esterases, potentially reducing available levels of the inhibitor to zero, plasma stabilities needed to be assessed. Cellular potencies and other physical data for selected proteasome inhibitors are shown in Table 5.

The remarkable ability of plasma esterases to hydrolyze hindered esters in buffered systems at neutral pH is demonstrated by the low plasma stabilities exhibited by all the hindered Glu esters (**17j**−**l**, **22c**, **22g**−**h**). After a 2 h incubation in human plasma, for example, only about half of the tetrapeptide vinyl sulfone *tert*-butyl ester **17j** and none of the corresponding cyclohexyl ester **17l** remained.[35] These results go a long way toward explaining the observed low cellular potencies of these compounds because hydrolysis would result in an inactive species. The success of the isostere approach in circumventing this problem can be seen by comparing ester **22g**, only 7% of

Table 4. SAR of Tripeptide 2-Keto-1,3,4-oxadiazoles

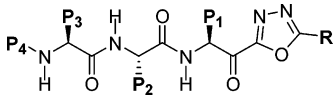

compd	P4	P3	P2	P1	R	ChT-L[a]	Tryp-L[b]	PGPH[c]	CatB[d]	CatS[e]
29a	mesyl	neopentylAsn	Ala	Leu	Ph	0.0057	nd[f]	nd	nd	nd
29b	*m*-tosyl	neopentylAsn	Ala	Leu	Ph	0.00065	>450	>450	nd	nd
29c	*p*-tosyl	neopentylAsn	Ala	Leu	Ph	0.00072	>300	>900	72	39
29d	*p*-tosyl	neopentylAsn	MeSer	Leu	Ph	0.00072	>900	>900	44	8.1
29e	*p*-tosyl	neopentylAsn	Ala	Aib	Ph	0.13	>450	>450	nd	nd
29f	DMS[17]	neopentylAsn	Ala	Leu	*i*-Pr	0.038	>900	>900	nd	nd
29g	*p*-tosyl	neopentylAsn	Ala	Leu	*p*-N(Me)$_2$Ph	0.00051	290	>300	nd	nd
29h	*p*-tosyl	neopentylAsn	MeSer	Leu	*p*-N(Me)$_2$Ph	0.0005	>300	>300	nd	nd
29i	*p*-tosyl	benzylSer	MeSer	Leu	Ph	0.032	51	>900	nd	nd
29j	*p*-tosyl	*o*-MebenzylSer	Ala	Leu	Ph	0.045	nd	nd	nd	nd
29k	*p*-tosyl	*m*-ClbenzylSer	Ala	Leu	Ph	0.14	nd	nd	nd	nd
29l	*p*-tosyl	*p*-MebenzylSer	Ala	Leu	Ph	0.5	nd	nd	nd	nd

[a] Ki_{app} (μM) for chymotrypsin-like proteasome activity. [b] Ki_{app} (μM) for trypsin-like proteasome activity. [c] Ki_{app} (μM) for post glutamyl peptide hydrolase-like proteasome activity. [d] Ki_{app} (μM) for cathepsin B activity. [e] Ki_{app} (μM) for cathepsin S activity. [f] Not determined.

Table 5. Properties of Selected Proteasome Inhibitors

compd	PC3 (nM)[a]	shift[b]	plasma stab. (%)[c]	PBS sol (μM)[d]
2	1	0.27	nd[e]	nd
3	375	>380	nd	nd
5b	600	160	nd	nd
10d	3000	860	100	nd
17a	800	12	66	nd
17c	600	22	22	<10
17e	450	9.2	83	nd
17h	3250	42	nd	nd
17j	2000	800	52	<10
17k	nd	nd	20	nd
17l	nd	nd	0	nd
17o	3000	58	89	nd
17p	5000	1600	89	57
17q	200	130	90	<10
17s	550	230	83	20
22a	7500	29	nd	nd
22b	1750	100	nd	nd
22c	6500	1100	1	<10
22e	3000	1000	nd	nd
22f	4000	3600	nd	nd
22g	500	240	7	48
22h	500	75	1	<10
22m	nd	nd	96	470
22n	2400	410	99	381
22o	nd	nd	100	500
29b	nd	nd	28	<10
29c	200	280	86	13
29d	nd	nd	79	37
29e	nd	nd	100	249
29g	nd	nd	72	<10

[a] IC_{50} for growth inhibitory effects in PC3 cells. [b] IC_{50} for PC3 cells/ Ki_{app} or IC_{50} for chymotrypsin-like proteasome activity. [c] Percent remaining in human plasma at 120 min, 37 °C. [d] Kinetic solubility in PBS at pH 7.4. [e] Not determined.

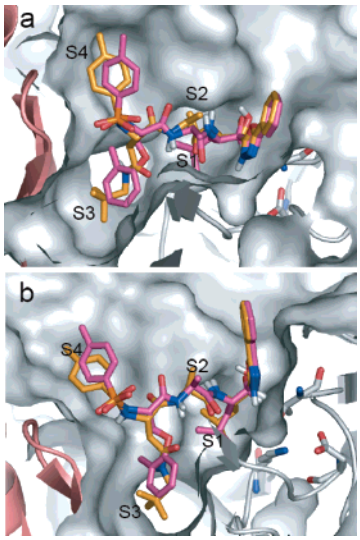

Figure 4. Top and side views of **29c** (orange) and **29j** (violet) docked into the β5 and β6 subunits of the bovine proteasome structure 1IRU using the MMF94 force field in MOE (Chemical Computing Group, Montreal, Quebec) as rendered in Pymol (DeLano Scientific, South San Francisco, CA).

which remains after 2 h in plasma, with its neopentyl Asn isostere **22m**, 96% of which remains under the same conditions. Only two other compounds (**17c**, **29b**) had stability problems that could not be attributed to ester hydrolysis, and no inherent differences in plasma stability between VSs and KODs were observed.

Solubilities, as expected, were poorest for the tetrapeptide vinyl sulfones and improved somewhat, as previously noted, for shorter compounds and *N*-terminal *p*-tosyl compounds. A comparison of the solubilities of VS **22m** (470 μM) and the analogous KOD **29c** (13 μM) reveals a propensity for lower solubilities with the latter, more hydrophobic phenyl-containing P1 electrophiles despite the fact that the electrophilic carbonyl group provides a potential site for reversible hydration and subsequent H-bonding with solvent.

A preliminary assessment of potential anticancer effects of these proteasome inhibitors was undertaken by examining the growth inhibitory effects of the compounds on PC3 cells, a human prostate cancer cell line, in a cellular assay from which a cytotoxic component cannot per se be excluded.[36] Whereas compounds tested had nanomolar or subnanomolar potencies in the in vitro enzyme assay, cellular IC_{50} values were often micromolar with the most notable exception being epoxomicin **2**. This compound, remarkably, showed cell growth inhibitory effects at a concentration below its IC_{50} value for the isolated enzyme, the explanation for which requires further study. Other submicromolar IC_{50} values were obtained with compounds such as VS **17q** and KOD **29c**, both having a value of 200 nM in this cellular assay.

For some of the compounds (e.g., **17j**, **22c**), the magnitude of the resulting shift, defined as the cellular IC_{50} value divided by the isolated enzyme inhibition constant, can be accounted for in terms of plasma instability, which reduces the concentration of the active component over the long time course of the

experiment. In other cases, the reason the inhibitor needed to be present at such high concentrations to have a cellular effect was less apparent. Lack of cell permeability is the most likely explanation, and in that context it was noted that none of the P3 Ser compounds (**22e**, **22f**, **22n**) had submicromolar cellular activity, perhaps implicating the additional −OH group in cell impermeability. Cellular efflux by active transporters such as P-gp, a mechanism which has been previously demonstrated to extrude one VS from intestinal cells,[37] is another possible explanation for the observed shifts. Additional experiments would be required to determine whether this is the case. Attempts to correlate observed cellular IC_{50} values for plasma stable compounds with enzyme potency, MW, cLogP, TPSA, the number of rotatable bonds, or combinations thereof met with little success. Empirically, the P3 neopentyl Asn isostere fared relatively well in the cellular assay, with tetrapeptide VS **17q** and KOD **29c**, both having IC_{50} values of 200 nM, being the best in each class.

Conclusions

Optimization of binding interactions between the β5 subunit of the human 20S proteasome and small, peptide-like VS inhibitors **10a**−**d**, **17a**−**t**, and **22a**−**o** uncovered key interactions at the S3 and S4 subsites, many of which agreed with modeling predictions. Most critical for optimal binding was a relatively linear P3 side chain that terminated with a large, hydrophobic substituent, such as *tert*-butyl Glu. Lack of solubility and plasma instabilities for such esters triggered a search for more favorable isosteres, which resulted in the selection of the neopentyl Asn side chain at P3. As shown in Figure 4, this moiety afforded a relatively tight fit with the cleft that constitutes the S3 subsite of the proteasome β5 subunit. Attempts to optimize a second series of P3 substituents, P3 benzyl serine ethers such as **17e**, led to less potent compounds.

Inhibitors could be made smaller by replacing the Cbz isoleucine *N*-terminus found in compounds **17** with a simpler aryl substituent interacting at S4. In practice, the *p*-toluenesulfonyl group or its analogues used in **22m**−**o** were found to be optimal. Substituent effects at P2 also played a definite role in compound activity, possibly because of conformational effects. Out of concern for keeping the molecular weights low, most inhibitors retained an unoptimized alanine at this position, although P2 serine and its methyl ether were also used in some analogues.

Optimal substituents at all positions were grafted onto a newly discovered warhead for proteasomes, 2-keto-1,3,4-oxadiazoles, to give remarkably potent, selective, and reversible inhibitors such as the 720 pM **29c**, thus demonstrating just how transferable the SAR was between the VS series and the later KODs. The vinyl sulfone SAR, in turn, had correlated well with what had previously been observed for aldehydes, providing evidence that all three series, as expected, utilize the same mode of binding with the enzyme, with significant differences in geometry being limited to the P1 and P1′ positions.

Optimization was accelerated through the concurrent measurement of enzymatic, physical, and cellular properties of the inhibitors, an approach, which more and more, is found to be necessary for timely drug discovery and development. Results from these studies combined with modeling considerations and a starting point based on a comparison of previously known proteasome inhibitors led to the discovery of novel, reversible 2-keto-1,3,4-oxadiazoles such as **29c** that could serve as key tool compounds for cellular and animal studies as well as provide a springboard for further optimization.

Experimental Section

General Procedures. Reagents and solvents were obtained from commercial sources and were used without purification. Flash chromatography was performed on 230−400 mesh silica gel (E. M. Science). Melting points were obtained on a Mel-Temp 3.0 melting point apparatus and are uncorrected. NMR spectra were recorded at the specified frequencies in DMSO-d_6 unless otherwise stated and were referenced to TMS. The following abbreviations were used: s, singlet; d, doublet; dd, doublet of doublets, etc.; m, multiplet; q, quartet; and b, broad. Mass spectra were obtained using PE Sciex API 150EX instruments in electrospray positive and negative ionization modes. HPLC homogeneities were determined using the specified reverse phase conditions. System A: Varian Polaris C18-A column (5 μm, 5 × 20 mm), 10−99% MeOH (+ 0.1% HCO_2H) in 0.1% HCO_2H, linear gradient in 12 min, then 2 min isocratic, and 1.5 mL/min flow rate with UV detection at 214 nM. System B: Phenomenex Prodigy C-18 ODS3 column (5 μm, 4.6 × 100 mm), 1−99% ACN (+ 0.1% TFA) in 0.1% TFA, linear gradient in 12 min, then 2 min isocratic, and 1.5 mL/min flow rate with UV detection at 214 nM. Elemental analyses were performed by Robertson Microlit Laboratories, Madison, NJ. Unless otherwise stated, the reactions were conducted at room temperature under an atmosphere of dry nitrogen.

Boc-LeuVSMe (7). Compound **6**[19] (5.48 g, 23.8 mmol) was dissolved in anhydrous THF (200 mL), cooled in an ice bath, and vigorously stirred. Sodium hydride was added in portions as a 60% mineral oil dispersion (1.10 g, 27.5 mmol). When the addition was complete and no more gas evolution was observed, a solution of Boc leucinal (5.12 g, 23.8 mmol), which had been made by the procedure of Falkiewicz, et al.,[38] in dry THF (50 mL) was added. After 30 min of vigorous stirring, 1 M HCl (50 mL) was carefully added, followed by the addition of EtOAc (100 mL). The phases were separated. The organic phase was washed with 1 M HCl, saturated $NaHCO_3$, and brine, and then dried over $MgSO_4$. Filtration and solvent evaporation left 8.0 g of a yellow oil that was flash chromatographed on silica gel using 20% EtOAc in hexane. Crude **7** (5.76 g) was obtained. This contained a small amount of **6** by LCMS analysis, but was suitable for use in the next step without further purification.

H-LeuVSMe Hydrochloride (8). Compound **7** (5.75 g crude) and 4.0 M HCl in 1,4-dioxane (50 mL) were stirred together. After 1 h, Et_2O (100 mL) was added. The reaction mixture was filtered. The precipitate was rinsed with a little more Et_2O and dried. Compound **8** (4.33 g) was obtained as a white solid, an 80% yield for the two steps. ^{1}H NMR (400 MHz): δ 8.59 (bs, 3H), 7.14 (d, J = 15.2 Hz, 1H), 6.69 (dd, J = 15.2, 8.0 Hz, 1H), 3.98 (m, 1H), 3.07 (s, 3H), 1.61 (m, 3H), 0.91 (m, 6H). MS *m*/*z*: 192 $(MH)^+$.

Ac-hPhe-Leu-Gly-LeuVSMe (10a). Mixed Anhydride Coupling. [2-(*S*)-(2-(*S*)-Acetylamino-4-phenyl-butyrylamino)-4-methyl-pentanoylamino]-acetic acid (117 mg, 0.30 mmol) was dissolved in 5 mL of anhydrous THF and stirred in an ice/methanol bath. *N*-Methylmorpholine (50 μL, 0.45 mmol) and then IBCF[17] (39 μL, 0.30 mmol) were added. After 10 min, compound **8** (68 mg, 0.30 mmol) was added as a solid, followed by the addition of NMM (50 μL, 0.45 mmol). After 30 min, the cold reaction mixture was poured into 0.2 M HCl and extracted twice with CH_2Cl_2. The combined organics were washed with water, saturated $NaHCO_3$, and brine and then dried over $MgSO_4$. Filtration and solvent evaporation followed by flash chromatography on silica gel using 5% MeOH/CH_2Cl_2 gave 88 mg of **10a** (52%) as a white solid. ^{1}H NMR (270 MHz): δ 8.20 (t, J = 5.7 Hz, 1H), 8.06 (t, J = 6.9 Hz, 2H), 7.83 (d, J = 7.9 Hz, 1H), 7.22 (m, 5H), 6.71 (m, 2H), 4.56 (m, 1H), 4.23 (m, 2H), 3.71 (ABX m, 2H), 2.97 (s, 3H), 2.58 (m, 2H), 1.88 (s, 3H), 1.3−1.8 (m, 8H), 0.83 (m, 12H). MS *m*/*z*: 565 $(MH)^+$. Anal. ($C_{28}H_{44}N_4O_6S$) C, H, N.

Ac-hPhe-Leu-Ala-LeuVSMe (10b). Using the same procedure described for the preparation of **10a** but starting with **9b**, a 41% yield of **10b** was obtained as a white solid. ^{1}H NMR (270 MHz): δ 8.14 (d, J = 7.4 Hz, 1H), 7.97 (d, J = 7.7 Hz, 2H), 7.88 (d, J = 8.4 Hz, 1H), 7.27 (m, 2H), 7.18 (m, 3H), 6.64 (m, 2H), 4.52 (m,

1H), 4.23 (m, 3H), 2.98 (s, 3H), 2.56 (m, 2H), 1.88 (s, 3H), 1.3−1.8 (m, 8H), 1.22 (d, J = 6.9 Hz, 3H), 0.83 (m, 12H). MS *m*/*z*: 579 $(MH)^+$. Anal. ($C_{29}H_{46}N_4O_6S$) C, H, N.

Ac-hPhe-Leu-(*D*)-Ala-LeuVSMe (10c). Using the same procedure described for the preparation of **10a** but starting with **9c**, a 31% yield of **10c** was obtained as a white solid. ^{1}H NMR (270 MHz): δ 8.10 (m, 3H), 7.91 (d, J = 8.4 Hz, 1H), 7.22 (m, 5H), 6.72 (m, 2H), 4.53 (m, 1H), 4.22 (m, 3H), 2.95 (s, 3H), 2.58 (m, 2H), 1.88 (s, 3H), 1.3−1.8 (m, 8H), 1.21 (d, J = 7.2 Hz, 3H), 0.82 (m, 12H). MS *m*/*z*: 579 $(MH)^+$. Anal. ($C_{29}H_{46}N_4O_6S$) C, H, N.

Ac-hPhe-Leu-Phe-LeuVSMe (10d). Using the same procedure described for the preparation of **10a** but starting with **9d**, a 61% yield of **10d** was obtained as a white solid. ^{1}H NMR (270 MHz): δ 8.09 (t, J = 7.9 Hz, 2H), 7.97 (d, J = 8.7 Hz, 1H), 7.92 (d, J = 7.9 Hz, 1H), 7.15 (m, 10H), 6.56 (dd, J = 15.2, 4.7 Hz, 1H), 6.25 (d, J = 15.2 Hz, 1H), 4.48 (m, 2H), 4.21 (m, 2H), 2.90 (s, 3H), 2.75−3.0 (m, 2H), 2.54 (m, 2H), 1.87 (s, 3H), 1.81 (m, 2H), 1.51 (m, 2H), 1.34 (m, 4H), 0.78 (m, 12H). MS *m*/*z*: 655 $(MH)^+$. Anal. ($C_{35}H_{50}N_4O_6S$) C, H, N.

Boc-Ala-LeuVSMe (12a). Boc-L-alanine (1.66 g, 8.77 mmol) and NMM (0.96 mL, 8.77 mmol) were dissolved in 50 mL of anhydrous THF and cooled to −10 °C under an inert atmosphere. IBCF (1.14 mL, 8.77 mmol) was added via syringe. After 5 min, **8** (2.00 g, 8.77 mmol) was added as a solid, followed by the addition of more NMM (0.96 mL, 8.77 mmol). After 1 h, the reaction was quenched with 1 M HCl and extracted three times with EtOAc. The combined extract was washed with 1 M HCl, saturated $NaHCO_3$, and brine. Drying, filtration, and solvent evaporation, followed by trituration with Et_2O/hexane gave 2.1 g of the product as a white solid (66% yield). ^{1}H NMR (400 MHz): δ 7.93 (d, J = 8.0 Hz, 1H), 6.94 (d, J = 7.2 Hz, 1H), 6.69 (dd, J = 15.6, 5.2 Hz, 1H), 6.60 (d, J = 15.6 Hz, 1H), 4.57 (m, 1H), 3.91 (m, 1H), 2.98 (s, 3H), 1.62 (m, 1H), 1.45 (m, 2H), 1.38 (s, 9H), 1.24 (d, J = 8.0 Hz, 3H), 0.85 (m, 6H). MS *m*/*z*: 385 $(m + Na)^+$.

H-Ala-LeuVSMe Hydrochloride (13a). Compound **12a** (1.80 g, 50 mmol) was stirred with 4 M HCl in 1,4-dioxane (125 mL, 500 mmol) for 1 h. Ether (200 mL) was added with vigorous stirring. The reaction mixture was filtered and the precipitate washed with more ether. The product (1.45 g) was obtained as a white solid (97% yield). ^{1}H NMR (400 MHz): δ 8.82 (d, J = 8.0 Hz, 1H), 8.31 (broad s, 3H), 6.72 (s, 2H), 4.57 (m, 1H), 3.91 (m, 1H), 3.03 (s, 3H), 1.69 (m, 1H), 1.35−1.54 (m, 2H), 1.44 (d, J = 6.8 Hz, 3H), 0.93 (d, J = 6.8 Hz, 3H), 0.89 (d, J = 6.8 Hz, 3H). MS *m*/*z*: 263 $(MH)^+$.

H-Ser-LeuVSMe Trifluoroacetate (13b). ^{1}H NMR (400 MHz): δ 8.57 (d, J = 8.0 Hz, 1H), 8.16 (broad s, 3H), 6.72 (s, 2H), 4.59 (broad q, J = 6.8 Hz, 1H), 3.6−3.9 (m, 2H), 3.77 (t, J = 6.8 Hz, 1H), 2.99 (s, 3H), 1.65 (m, 1H), 1.45 (m, 2H), 0.90 (d, J = 6.8 Hz, 3H), 0.87 (d, J = 6.8 Hz, 3H). MS *m*/*z*: 279 $(MH)^+$.

H-Aib-LeuVSMe Hydrochloride (13c). ^{1}H NMR (400 MHz): δ 8.45 (d, J = 8.4 Hz, 1H), 8.23 (broad s, 3H), 6.70 (dd, J = 15.2, 4.8 Hz, 1H), 6.63 (d, J = 15.2 Hz, 1H), 4.65 (m, 1H), 3.04 (s, 3H), 1.60 (s, 3H), 1.47 (s, 3H), 1.4−1.7 (m, 3H), 0.93 (d, J = 5.6 Hz, 3H), 0.88 (d, J = 6.0 Hz, 3H). MS *m*/*z*: 299 $(m + Na)^+$.

Tetrapeptide Vinyl Sulfone Syntheses. Method A. Cbz-Ile-Glu(O*t*Bu)-OH (14j). Succinate Ester Coupling. Cbz-(*L*)-isoleucine succinate ester (2.17 g, 6.00 mmol) and (*L*)-glutamic acid γ-*tert*-butyl ester (1.22 g, 6.00 mmol) were dissolved in a mixture of THF (98 mL) and water (9 mL). Triethylamine (1.67 mL, 12.00 mmol) was added. The solution was stirred at ambient temperature for 14 h, then poured into 0.2 N aqueous HCl (200 mL), and extracted twice with CH_2Cl_2. The combined organic phase was washed with water and brine and then dried over anhyd Mg_2SO_4. Filtration and solvent evaporation afforded 2.5 g of foam. Trituration with ether/hexane gave 1.84 g of **14j** as a white powder (68% yield). ^{1}H NMR (270 MHz): δ 8.15 (d, J = 7.6 Hz, 1H), 7.35 (m, 6H), 5.02 (s, 2H), 4.22 (m, 1H), 3.89 (m, 1H), 2.26 (t, J = 7.9 Hz, 2H), 1.94 (m, 1H), 1.72 (m, 3H), 1.39 (s, 9H), 1.09 (m,1H), 0.83 (m, 6H). MS *m*/*z*: 449 $(M - H)^-$.

Cbz-Ile-Glu(O*t*Bu)-OSu (15j). Succinate Ester Preparation. Compound **14j** (1.73 g, 3.84 mmol) and *N*-hydroxysuccinimide (0.442 g, 3.84 mmol) were dissolved in 30 mL of dry THF and stirred under nitrogen at 5 °C. Molten DCC (0.792 g, 3.84 mmol) was poured in. After 14 h, the reaction mixture was chilled and filtered, and the filtrate was evaporated. Trituration with ether gave 2.06 g of a hard white solid (98% yield). Proton NMR analysis indicates that the product contained 6% (by weight) dicyclohexylurea (DCU), but the material was suitable for use without further purification. ^{1}H NMR (270 MHz): δ 8.64 (d, J = 7.2 Hz, 1H), 7.35 (m, 7H), 5.03 (s, 2H), 4.72 (m, 1H), 3.92 (t, J = 8.4 Hz, 1H), 2.81 (s, 4H), 2.50 (t, J = 2.0 Hz, 2H), 1.8−2.15 (m, 2H), 1.5−1.8 (m, 2H, includes DCU), 1.43 (s, 9H), 0.83 (m, 6H).

Cbz-Ile-Glu(O*t*Bu)-Ala-OH (16j). Succinate Ester Coupling Procedure. Compound **15j** (2.01 g, 3.67 mmol) was dissolved in 40 mL of dry THF. Triethylamine (0.51 mL, 7.34 mmol) was added, followed by L-alanine (0.327 g, 3.67 mmol) as a cloudy suspension in 5 mL of THF plus 5 mL of water. The addition of another 5 mL of water gave a clear, homogeneous reaction mixture at pH 5.5. Triethylamine was periodically added in 0.10 mL portions until the pH stabilized at 8.5. After 14.5 h, the reaction was poured into 200 mL of 0.5 M HCl and extracted twice with CH_2Cl_2. The combined organic phase was washed with water and brine and then dried over anhyd Mg_2SO_4. Filtration and solvent evaporation gave 1.9 g of a sticky white foam. Trituration with ether gave 1.35 g of **16j** as a white solid (71% yield). ^{1}H NMR (270 MHz): δ 8.17 (d, J = 7.2 Hz, 1H), 7.96 (d, J = 7.9 Hz, 1H), 7.35 (m, 6H), 5.02 (s, 2H), 4.30 (m, 1H), 4.16 (m, 1H), 3.90 (t, J = 8.4 Hz, 1H), 2.24 (t, J = 8.2 Hz, 2H), 1.55−1.95 (m, 3H), 1.39 (s, 9H), 1.25 (d, J = 7.2 Hz, 3H), 1.12 (m, 2H), 0.81 (m, 6H). MS *m*/*z*: 520 $(M - H)^-$.

Cbz-Ile-Glu(O*t*Bu)-Ala-LeuVSMe (17j). Mixed anhydride coupling was carried out using the general method given for the synthesis of **10a**. Starting with **16j** (261 mg, 0.50 mmol) and **8** (114 mg, 0.50 mmol), **17j** was obtained as a white solid (239 mg, 69% yield). ^{1}H NMR (270 MHz): δ 8.03 (m, 3H), 7.35 (m, 6H), 6.66 (m, 2H), 5.04 (s, 2H), 4.55 (m, 1H), 4.25 (m, 2H), 3.91 (t, J = 7.7 Hz, 1H), 2.99 (s, 3H), 2.22 (t, J = 8.2 Hz, 2H), 1.55−1.95 (m, 5H), 1.38 (s, 9H), 1.23 (d, J = 6.9 Hz, 3H), 1.0−1.2 (m, 2H), 0.83 (m, 12H). MS *m*/*z*: 696 $(M + H)^+$. HPLC homogeneity 97.0% (System A); 100% (System B).

Other Compounds Made Using Method A. Cbz-Ile-Leu-Ala-LeuVSMe (17a). ^{1}H NMR (270 MHz): δ 7.95 (m, 3H), 7.35 (m, 6H), 6.65 (m, 2H), 5.03 (s, 2H), 4.53 (m, 1H), 4.26 (m, 2H), 3.88 (t, J = 7.9 Hz, 1H), 2.99 (s, 3H), 1.3−1.8 (m, 7H), 1.22 (d, J = 7.2 Hz, 3H), 1.0−1.25 (m, 2H), 0.82 (m, 18H). MS *m*/*z*: 624 $(MH)^+$. Anal. ($C_{31}H_{50}N_4O_7S$) C, H, N.

Cbz-Ile-Phe-Ala-LeuVSMe (17b). ^{1}H NMR (400 MHz): δ 8.14 (d, J = 7 Hz, 1H), 7.97 (m, 2H), 7.32 (m, 6H), 7.22 (m, 5H), 6.65 (m, 2H), 5.02 (s, 2H), 4.54 (m, 2H), 4.24 (m, 1H), 3.80 (t, J = 8 Hz, 1H), 3.01 (m, 4H), 2.77 (m, 1H), 1.62 (m, 2H), 1.39 (m, 2H), 1.23 (d, J = 7 Hz, 4H), 1.02 (m, 1H), 0.83 (m, 6H), 0.74 (t, J = 7 Hz, 3H), 0.65 (d, J = 7 Hz, 3H). MS *m*/*z*: 658 $(MH)^+$. Anal. ($C_{34}H_{48}N_4O_7S$) C, H, N.

Cbz-Ile-hPhe-Ala-LeuVSMe (17c). ^{1}H NMR (400 MHz): δ 8.09 (d, J = 7.2 Hz, 1H), 8.00 (d, J = 10.0 Hz, 2H), 7.47 (d, J = 7.2 Hz, 1H), 7.2−7.4 (m, 10H), 6.65 (m, 2H), 5.03 (s, 2H), 4.53 (m, 1H), 4.26 (m, 2H), 3.93 (t, J = 7.2 Hz, 1H), 2.98 (s, 3H), 2.56 (m, 2H), 1.8−2.0 (m, 3H), 1.58 (m, 1H), 1.3−1.5 (m, 2H), 1.24 (d, J = 6.8 Hz, 3H), 1.15 (m, 2H), 0.85 (m, 12H). MS *m*/*z*: 671 $(MH)^+$. Anal. ($C_{35}H_{50}N_4O_7S$) C, H, N.

Cbz-Ile-*trans*-StyrylAla-Ala-LeuVSMe (17d). ^{1}H NMR (270 MHz, CD_3OD): δ 7.05−7.3 (m, 10H), 6.72 (dd, J = 15.4, 4.5 Hz, 1H), 6.54 (d, J = 15.4 Hz, 1H), 6.42 (d, J = 15.8 Hz, 1H), 6.14 (m, 1H), 4.94 (ABq, 2H), 4.55 (m, 1H), 4.32 (m, 1H), 4.21 (q, J = 7.2 Hz, 1H), 3.83 (d, J = 6.2 Hz, 1H), 2.87 (s, 3H), 2.65 (m, 1H), 2.53 (m, 1H), 1.2−1.8 (m, 5H), 1.30 (d, J = 7.4 Hz, 3H), 1.08 (m, 1H), 0.81 (m, 12H). MS *m*/*z*: 683 $(MH)^+$. HPLC homogeneity 95.0% (System A); 93.7% (System B).

Cbz-Ile-Ser(OBn)-Ala-LeuVSMe (17e). ^{1}H NMR (400 MHz): δ 8.07 (m, 2H), 7.81 (d, J = 8 Hz, 1H), 7.41 (d, J = 7 Hz, 1H), 7.30 (m, 10H), 6.62 (m, 2H), 5.02 (ABq, 2H), 4.56 (m, 1H), 4.50 (m, 1H), 4.48 (s, 2H), 4.24 (t, J = 7 Hz, 1H), 3.95 (t, J = 7 Hz, 1H), 3.62 (broad s, 2H), 2.97 (s, 3H), 1.75 (m, 1H), 1.56 (m, 1H),

1.0−1.45 (m, 4H), 1.23 (d, J = 7 Hz, 3H), 0.82 (m, 12H). MS m/z: 687 $(MH)^+$. HPLC homogeneity 94.7% (System A); 96.3% (System B).

Cbz-Ile-MetO_2-Ala-LeuVSMe (17f). ^{1}H NMR (400 MHz): δ 8.18 (d, J = 8.0 Hz, 1H), 8.13 (d, J = 6.8 Hz, 1H), 8.08 (d, J = 8.4 Hz, 1H), 7.45 (d, J = 8.4 Hz, 1H), 7.35 (m, 5H), 6.68 (dd, J = 15.2, 4.4 Hz, 1H), 6.62 (d, J = 15.2 Hz, 1H), 5.03 (s, 2H), 4.55 (m, 1H), 4.42 (q, J = 6.0 Hz, 1H), 4.22 (m, 1H), 3.90 (t, J = 7.6 Hz, 1H), 3.11 (m, 2H), 3.00 (s, 3H), 2.94 (s, 3H), 2.00 (m, 2H), 1.73 (m, 1H), 1.62 (m, 1H), 1.41 (m, 3H), 1.25 (d, J = 7.2 Hz, 3H), 1.13 (m, 1H), 0.83 (m, 12H). MS m/z: 674 $(MH)^+$. Anal. ($C_{30}H_{48}N_4O_9S_2$) C, H, N.

Compound 17g. ^{1}H NMR (400 MHz): δ 8.65 (d, J = 8.0 Hz, 1H), 8.31 (d, J = 6.8 Hz, 1H), 7.75 (d, J = 8.0 Hz, 1H), 7.52 (d, J = 7.6 Hz, 1H), 7.3−7.5 (m, 10H), 6.66 (dd, J = 15.2, 4.0 Hz, 1H), 6.61 (d, J = 15.2 Hz, 1H), 4.99 (ABq, 2H), 4.90 (m, 1H), 4.53 (m, 3H), 4.18 (m, 1H), 3.87 (t, J = 7.2 Hz, 1H), 3.61 (dd, J = 14.8, 6.0 Hz, 1H), 3.39 (m, 1H), 2.97 (s, 3H), 1.73 (m, 1H), 1.59 (m, 1H), 1.40 (m, 3H), 1.25 (d, J = 6.8 Hz, 3H), 1.12 (m, 1H), 0.83 (m, 12H). MS m/z: 736 $(MH)^+$. Anal. ($C_{35}H_{50}N_4O_9S_2$) C, H, N.

Cbz-Ile-Asp(OBn)-Ala-LeuVSMe (17i). ^{1}H NMR (400 MHz): δ 8.40 (d, J = 8.0 Hz, 1H), 7.94 (d, J = 6.8 Hz, 1H), 7.83 (d, J = 8.8 Hz, 1H), 7.42 (d, J = 8.0 Hz, 1H), 7.34 (m, 10H), 6.68 (dd, J = 15.4, 4.4 Hz, 1H), 6.60 (dd, J = 15.4, 1.2 Hz, 1H), 5.01 (m, 4H), 4.66 (q, J = 7.6 Hz, 1H), 4.54 (m, 1H), 4.19 (m, 1H), 3.88 (t, J = 7.6 Hz, 1H), 2.99 (s, 3H), 2.90 (dd, J = 16.4, 6.4 Hz, 1H), 2.70 (dd, J = 16.4, 8.0 Hz, 2H), 1.65 (m, 2H), 1.41 (m, 3H), 1.22 (d, J = 6.8 Hz, 2H), 1.11 (m, 1H), 0.83 (m, 12H). MS m/z: 716 $(MH)^+$. Anal. ($C_{36}H_{50}N_4O_9S$) C, H, N.

Cbz-Ile-CyclohexylGlu-Ala-LeuVSMe (17l). ^{1}H NMR (300 MHz): δ 8.07 (m, 3H), 7.44 (d, J = 9 Hz, 1H), 7.37 (s, 5H), 6.64 (m, 2H), 5.04 (s, 2H), 4.61 (m, 2H), 4.28 (m, 2H), 3.91 (t, J = 9 Hz, 1H), 3.00 (s, 3H), 2.30 (m, 2H), 1.55−2.0 (m, 8H), 1.1−1.55 (m, 10H), 1.22 (d, J = 7 Hz, 3H), 0.83 (m, 12H). MS m/z: 722 $(MH)^+$. Anal. ($C_{36}H_{56}N_4O_9S$) C, H, N.

Cbz-Ile-Gln-Ala-LeuVSMe (17m). ^{1}H NMR (270 MHz): δ 8.14 (J = 7.4 Hz, 1H), 7.95 (d, J = 6.9 Hz, 2H), 7.37 (m, 6H), 7.23 (broad s, 1H), 6.78 (broad s, 1H), 6.65 (m, 2H), 5.03 (d, J = 2.5 Hz, 2H), 4.55 (m, 1H), 4.22 (m, 2H), 3.89 (t, J = 7.7 Hz, 1H), 2.99 (s, 3H), 2.11 (t, J = 7.7 Hz, 2H), 1.3−1.9 (m, 7H), 1.22 (d, J = 6.9 Hz, 3H), 1.0−1.2 (m, 1H), 0.85 (m, 12H). MS m/z: 639 $(MH)^+$. Anal. ($C_{30}H_{47}N_5O_8S$) C, H, N.

Method B. Boc-NeopentylAsn-O-*t*-Bu (19q). Side Chain Coupling with EDC/HOAt. To a stirred solution of Boc-Asp-α-*tert*-butyl ester (3.00 g, 10.4 mmol) and *N*-methylmorpholine (2.3 mL, 21 mmol) in dry DMF (50 mL) were added EDC (2.00 g, 10.4 mmol) and HOAt (0.14 g, 1.04 mmol). After 15 min, neopentylamine (1.40 mL, 12.0 mmol) was added. After 4 h, 1 M HCl (150 mL) was added, and the mixture plus 100 mL of ether was transferred to a separatory funnel. The organic phase was separated, and the aqueous phase was washed with more ether. The combined organic phase was washed with water, saturated $NaHCO_3$, and brine. Drying over $MgSO_4$ followed by concentration gave 3.21 g, a 90% yield, of **19q** as a colorless syrup that slowly crystallized. ^{1}H NMR (400 MHz, $CDCl_3$): δ 5.72 (broad d, 2H), 4.36 (m, 1H), 3.05 (d, J = 6.6 Hz, 2H), 2.77 (ABm, 2H), 1.48 (s, 9H), 1.46 (s, 9H), 0.92 (s, 9H). MS m/z: 359 $(MH)^+$.

β-Neopentylasparagine Hydrochloride (20q). Compound **19q** (1.20 g, 3.48 mmol) was dissolved in 4 M HCl in 1,4-dioxane (10 mL, 40 mmol). After 2 h, the reaction mixture was concentrated by rotary evaporation in the presence of several portions of toluene. Ether was added, and the white solid was filtered and vacuum-dried. Compound **20q (**0.82 g, 99%) was obtained. ^{1}H NMR (400 MHz, $CDCl_3$): δ 8.32 (broad s, 3H), 8.15 (s, 1H), 4.13 (broad s, 1H), 2.80 (m, 2H), 2.52 (s, 2H), 0.83 (s, 9H). MS m/z: 203 $(MH)^+$.

Cbz-Ile-NeopentylAsn-OH (14q). Coupling of **20q** with Cbz-Ile-OSu using the procedure described for the preparation of **16j** afforded dipeptide **14q** in a 47% yield. ^{1}H NMR (400 MHz): δ 12.6 (broad s, 1H), 8.12 (d, J = 7.6 Hz, 1H), 7.83 (broad t, J = 5.6 Hz, 1H), 7.52 (d, J = 8.4 Hz, 1H), 7.35 (m, 5H), 5.04 (s, 2H), 4.55 (q, J = 6.8 Hz, 1H), 3.92 (m, 1H), 2.88 (d, J = 5.6 Hz, 2H), 2.61 (dd, overlaps with HOD, J = 15.2, 5.6 Hz, 2H), 1.0−1.8 (m, 3H), 0.84 (m, 15H). MS m/z: 448 $(M - H)^-$.

Cbz-Ile-NeopentylAsn-Ala-LeuVSMe (17q). Mixed anhydride coupling of **14q** with **13a** using the general procedure outlined for **10a** gave **17q** in a 71% yield. ^{1}H NMR (400 MHz): δ 8.35 (d, J = 7.2 Hz, 1H), 8.17 (d, J = 7.6 Hz, 1H), 8.10 (d, J = 8.4 Hz, 1H), 8.07 (t, J = 6.4 Hz, 1H), 7.41 (d, J = 8.0 Hz, 1H), 7.36 (m, 5H), 6.65 (dd, J = 15.2, 4.0 Hz, 1H), 6.60 (d, J = 15.2 Hz, 1H), 5.03 (ABq, 2H), 4.55 (m, 2H), 4.10 (m, 1H), 3.90 (t, J = 8.0 Hz, 1H), 2.92 (s, 3H), 2.87 (m, 2H), 2.70 (m, 1H), 2.55 (m, 1H), 1.5−1.75 (m, 3H), 1.41 (m, 2H), 1.25 (d, J = 7.2 Hz, 3H), 1.12 (m, 1H), 0.89 (d, J = 6.4 Hz, 3H), 0.84 (d, J = 6.4 Hz, 3H), 0.81 (m, 15 H). gCOSY NMR shows coupling between peaks at δ 1.25 (Ala CH_3) and δ 4.10 (Ala C*H*), δ 3.90 (Ile C*H*) and δ 7.41 (Ile N*H*), and between peaks at δ 2.87 (HNCH_2*t*-Bu) and δ 8.07 (*H*NCH_2*t*-Bu). MS m/z: 694 $(MH)^+$. Anal. ($C_{34}H_{55}N_5O_8S$) C, H, N.

Other Compounds Made Using Method B. Cbz-Ile-Asp-(O*t*Bu)-Ala-LeuVSMe (17h). ^{1}H NMR (400 MHz): δ 8.32 (d, J = 7.6 Hz, 1H), 7.90 (d, J = 6.8 Hz, 1H), 7.85 (d, J = 8.4 Hz, 1H), 7.42 (d, J = 8.0 Hz, 1H), 7.35 (m, 5H), 6.67 (dd, J = 15.2, 4.4 Hz, 1H), 6.60 (d, J = 15.2 Hz, 1H), 5.02 (ABq, 2H), 4.56 (m, 2H), 4.20 (m, 1H), 3.87 (t, J = 7.0 Hz, 1H), 2.98 (s, 3H), 2.73 (dd, J = 16.8, 5.6 Hz, 1H), 2.51 (m, overlaps with DMSO, 1H), 1.5−1.8 (m, 2H), 1.42 (m, 2H), 1.37 (s, 9H), 1.22 (d, J = 6.8 Hz, 3H), 1.12 (m, 2H), 0.83 (m, 12H). MS m/z: 682 $(MH)^+$. Anal. ($C_{33}H_{52}N_4O_9S$) C, H, N.

Cbz-Ile-*t*-ButylhomoGlu-Ala-LeuVSMe (17k). ^{1}H NMR (270 MHz): δ 7.97 (m, 3H), 7.35 (m, 6H), 6.65 (m, 2H), 5.03 (s, 2H), 4.53 (m, 1H), 4.24 (m, 2H), 3.89 (t, J = 7.9 Hz, 1H), 2.99 (s, 3H), 2.14 (broad t, J = 6.0 Hz, 2H), 1.0−1.8 (m, 10H), 1.41 (s, 9H), 1.24 (d, J = 7.0 Hz, 3H), 0.83 (m, 12H). MS m/z: 709 $(MH)^+$. Anal. ($C_{35}H_{56}N_4O_9S$) C, H, N.

Cbz-Ile-hGln-Ala-LeuVSMe (17n). ^{1}H NMR (400 MHz): δ 8.00 (m, 4H), 7.36 (m, 5H), 7.21 (broad s, 1H), 6.73 (broad s, 1H), 6.65 (ABq, 2H), 5.03 (ABq, 2H), 4.54 (m, 1H), 4.22 (m, 2H), 3.89 (t, J = 7.6 Hz, 1H), 2.99 (s, 3H), 2.02 (broad t, J = 6.4 Hz, 2H), 1.3−1.8 (m, 10H), 1.22 (d, J = 7.2 Hz, 3H), 1.0−1.3 (m, 2H), 0.83 (m, 12H). MS m/z: 652 $(MH)^+$. Anal. ($C_{31}H_{49}N_5O_8S\cdot H_2O$) C, H, N.

Cbz-Ile-*i*PrGln-Ala-LeuVSMe (17o). ^{1}H NMR (300 MHz): δ 8.26 (d, J = 8 Hz, 1H), 8.04 (m, 2H), 7.85 (d, J = 8 Hz, 1H), 7.49 (d, J = 7 Hz, 1H), 7.36 (m, 5H), 6.67 (m, 2H), 5.05 (s, 2H), 4.54 (m, 1H), 4.23 (m, 2H), 3.88 (m, 1H), 2.97 (s, 3H), 2.11 (broad t, J = 7 Hz, 2H), 1.3−2.0 (m, 9H), 1.24 (d, J = 7 Hz, 3H), 1.03 (d, J = 6 Hz, 6H), 0.86 (m, 12H). MS m/z: 681 $(MH)^+$. HPLC homogeneity 96.1% (System A); 91.0% (System B).

Cbz-Ile-*t*-ButylGln-Ala-LeuVSMe (17p). ^{1}H NMR (300 MHz): δ 8.16 (d, J = 8 Hz, 1H), 8.09 (m, 1H), 7.97 (m, 2H), 7.45 (d, J = 8 Hz, 1H), 7.33 (m, 5H), 6.66 (m, 2H), 5.05 (s, 2H), 4.56 (m, 1H), 4.23 (m, 2H), 3.90 (t, J = 7 Hz, 1H), 2.98 (s, 3H), 2.09 (broad t, J = 7 Hz, 2H), 1.5−2.0 (m, 3H), 1.40 (m, 3H), 1.21 (m, 14H), 0.83 (m, 12H). MS m/z: 695 $(MH)^+$. Anal. ($C_{34}H_{55}N_5O_8S$) C, H, N.

Cbz-Ile-NeopentylGln-Ala-LeuVSMe (17r). ^{1}H NMR (400 MHz): δ 8.16 (d, J = 7.6 Hz, 1H), 7.96 (d, J = 8.0 Hz, 2H), 7.69 (t, J = 6.4 Hz, 1H), 7.43 (d, J = 8.4 Hz, 1H), 7.36 (m, 5H), 5.04 (ABq, 2H), 4.54 (m, 1H), 4.23 (m, 2H), 3.89 (t, J = 7.2 Hz, 1H), 2.99 (s, 3H), 2.87 (m, 2H), 2.18 (broad t, J = 7.2 Hz, 2H), 1.65−1.95 (m, 4H), 1.60 (m, 1H), 1.41 (m, 3H), 1.22 (d, J = 7.2 Hz, 3H), 1.13 (m, 2H), 0.82 (m, 21H). MS m/z: 709 $(MH)^+$. Anal. ($C_{35}H_{57}N_5O_8S$) C, H, N.

Compound 17s. ^{1}H NMR (300 MHz): δ 8.16 (d, J = 8 Hz, 1H), 7.95 (m, 2H), 7.45 (d, J = 8 Hz, 1H), 7.38 (s, 5H), 7.20 (s, 1H), 6.65 (m, 2H), 5.03 (s, 2H), 4.57 (m, 1H), 4.23 (m, 2H), 3.91 (t, J = 7 Hz, 1H), 3.00 (s, 3H), 2.12 (bt, J = 7 Hz, 2H), 1.5−1.9 (m, 6H), 1.42 (m, 4H), 1.22 (d, J = 7 Hz, 3H), 1.15 (d, J = 5 Hz, 6H), 0.83 (m, 15H). MS m/z: 709 $(MH)^+$. Anal. ($C_{35}H_{57}N_5O_8S$) C, H, N.

Cbz-Ile-Pro-Ala-LeuVSMe (17t). ^{1}H NMR (400 MHz): δ 7.99 (d, J = 7.6 Hz, 1H), 7.87 (d, J = 8.4 Hz, 1H), 7.54 (d, J = 8.8 Hz,

1H), 7.33 (m, 6H), 6.66 (s, 2H), 5.01 (ABq, 2H), 4.55 (m, 1H), 4.32 (m, 1H), 4.15 (m, 1H), 4.07 (t, J = 8.4 Hz, 1H), 3.74 (m, 1H), 3.60 (m, 1H), 2.97 (s, 3H), 2.04 (m, 1H), 1.65−1.95 (m, 4H), 1.30−1.65 (m, 3H), 1.26 (d, J = 6.8 Hz, 3H), 1.0−1.3 (m, 1H), 0.83 (m, 12H). MS *m*/*z*: 608 $(MH)^+$. Anal. ($C_{30}H_{46}N_4O_7S\cdot0.5\ H_2O$) C, H, N.

Tripeptide Vinyl Sulfone Syntheses. *p*Tosyl-NeopentylAsn-OH (21). Compound **20q** (1.50 g, 6.28 mmol) was dissolved in THF (15 mL) and 1.0 N NaOH (15 mL) and then cooled in an ice bath. *p*-Toluenesulfonyl chloride (1.20 g, 6.28 mmol) was added portionwise to the vigorously stirred solution. The pH of the reaction mixture was frequently adjusted to >8 by the addition of 4 M NaOH. After 2 h, the mixture was acidified with 6 M HCl and extracted thrice with EtOAc. The combined organic phase was washed with 1 M HCl, water, and brine and then dried over $MgSO_4$. Filtration and solvent evaporation followed by vacuum-drying gave **21** (2.24 g, 60%) as a white solid, mp 163.5−165 °C. ^{1}H NMR (400 MHz): δ 12.55 (broad s, 1H), 7.89 (d, J = 8.4 Hz, 1H), 7.71 (t, J = 6.0 Hz, 1H), 7.62 (d, J = 8.0 Hz, 2H), 7.31 (d, J = 8.0 Hz, 2H), 4.09 (q, J = 7.2 Hz, 1H), 2.79 (m, 2H), 2.50 (m, overlaps with DMSO, 1H), 2.36 (s, 3H), 2.28 (dd, J = 15.2, 6.0 Hz, 1H), 0.78 (s, 9H).

***p*Tosyl-NeopentylAsn-Ser-LeuVSMe (22n).** Compound **21** was coupled with **13b** using the standard mixed anhydride protocol described above for the preparation of **10a**. For **22n**, a white solid: ^{1}H NMR (400 MHz): δ 8.22 (d, J = 6.0 Hz, 1H), 8.05 (m, 3H), 7.63 (d, J = 7.8 Hz, 2H), 7.31 (d, J = 7.8 Hz, 2H), 6.59 (dd, J = 15.2, 4.0 Hz, 1H), 6.52 (d, J = 15.2 Hz, 1H), 4.50 (m, 1H), 4.10 (m, 1H), 3.62 (m, 2H), 3.35 (m, obscured by H_2O, 2H), 2.86 (s, 3H), 2.7−2.9 (m, 2H), 2.61 (m, 1H), 2.40 (m, 1H), 2.38 (s, 3H), 1.62 (m, 1H), 1.55 (m, 1H), 1.37 (m, 1H), 0.85 (d, J = 6.8 Hz, 3H), 0.81 (d, J = 6.8 Hz, 3H), 0.78 (s, 9H). MS *m*/*z*: 617 $(MH)^+$. Anal. ($C_{27}H_{44}N_4O_8S_2$) C, H, N.

Ac-Glu(O*t*Bu)-Ala-LeuVSMe (22a). ^{1}H NMR (300 MHz): δ 8.12 (d, J = 7 Hz, 1H), 8.09 (d, J = 8 Hz, 1H), 7.98(d, J = 9 Hz, 1H), 6.66 (m, 2H), 4.55 (m, 1H), 4.23 (m, 2H), 3.00 (s, 3H), 2.22 (t, J = 7 Hz, 2H), 1.85 (s, 3H), 1.5−1.9 (m, 3H), 1.38 (s, 9H), 1.1−1.5 (m, 2H), 1.24 (d, J = 7 Hz, 3H), 0.85 (m, 6H). MS *m*/*z*: 490 $(MH)^+$. Anal. ($C_{22}H_{39}N_3O_7S$) C, H, N.

Benzoyl-Glu(O*t*Bu)-Ala-LeuVSMe (22b). ^{1}H NMR (400 MHz): δ 8.49 (d, J = 7.6 Hz, 1H), 8.15 (d, J = 7.2 Hz, 1H), 7.94 (d, J = 8.8 Hz, 1H), 7.87 (d, J = 8.0 Hz, 2H), 7.53 (m, 1H), 7.45 (m, 2H), 6.64 (m, 2H), 4.53 (m, 1H), 4.38 (m, 1H), 4.25 (m, 1H), 2.99 (s, 3H), 2.32 (broad t, J = 8.0 Hz, 2H), 1.8−2.1 (m, 2H), 1.59 (m, 1H), 1.34 (s, 9H), 1.3−1.5 (m, 2H), 1.24 (d, J = 7.2 Hz, 3H), 0.83 (m, 6H). MS *m*/*z*: 552 $(MH)^+$. Anal. ($C_{27}H_{41}N_3O_7S$) C, H, N.

Cbz-Glu(O*t*Bu)-Ala-LeuVSMe (22c). ^{1}H NMR (400 MHz): δ 8.09 (d, J = 7.6 Hz, 1H), 8.01 (d, J = 8.8 Hz, 1H), 7.48 (d, J = 8.0 Hz, 1H), 7.33 (m, 5H), 6.65 (m, 2H), 5.01 (ABq, 2H), 4.54 (m, 1H), 4.24 (m, 1H), 4.00 (m, 1H), 2.99 (s, 3H), 2.23 (broad t, J = 8.0 Hz, 2H), 1.84 (m, 1H), 1.5−1.8 (m, 2H), 1.38 (s, 9H), 1.23 (d, J = 7.0 Hz, 3H), 1.1−1.5 (m, 2H), 0.84 (m, 6H). MS *m*/*z*: 604 $(M + Na)^+$. Anal. ($C_{28}H_{43}N_3O_8S$) C, H, N.

Cbz-Glu(O*t*Bu)-Gly-LeuVSMe (22d). ^{1}H NMR (400 MHz): δ 8.25 (broad t, J = 5.6 Hz, 1H), 7.85 (d, J = 8.0 Hz, 1H), 7.60 (d, J = 5.6 Hz, 1H), 7.32 (m, 5H), 6.69 (m, 2H), 5.02 (ABq, 2H), 4.57 (m, 1H), 3.99 (m, 1H), 3.73 (m, 2H), 2.98 (s, 3H), 2.25 (broad t, J = 7.2 Hz, 2H), 1.88 (m, 1H), 1.74 (m, 1H), 1.59 (m, 1H), 1.38 (s, 9H), 1.3−1.5 (m, 2H), 0.86 (m, 6H). MS *m*/*z*: 566 $(M - H)^-$. Anal. ($C_{27}H_{41}N_3O_8S$) C, H, N.

Cbz-Glu(O*t*Bu)-Ser-LeuVSMe (22e). ^{1}H NMR (400 MHz): δ 8.04 (d, J = 8.0 Hz, 1H), 7.94 (d, J = 7.2 Hz, 1H), 7.52 (d, J = 6.8 Hz, 1H), 7.32 (m, 5H), 6.69 (broad s, 2H), 5.02 (m, 3H), 4.57 (m, 1H), 4.27 (m, 1H), 4.04 (m, 1H), 3.59 (broad s, 2H), 2.96 (s, 3H), 2.23 (broad t, J = 7.2 Hz, 2H), 1.84 (m, 1H), 1.5−1.8 (m, 2H), 1.38 (s, 9H), 1.2−1.5 (m, 2H), 0.84 (m, 6H). MS *m*/*z*: 596 $(M - H)^-$. Anal. ($C_{28}H_{43}N_3O_9S$) C, H, N.

Benzenesulfonyl-Glu(O*t*Bu)-Ser-LeuVSMe (22f). ^{1}H NMR (400 MHz): δ 8.02 (d, J = 6.8 Hz, 3H), 7.74 (d, J = 7.6 Hz, 2H), 7.54 (m, 3H), 6.66 (m, 2H), 5.03 (t, J = 9.2 Hz, 1H), 4.55 (m, 1H), 4.03 (m, 1H), 3.79 (m, 1H), 3.39 (m, 2H), 2.95 (s, 3H), 2.09 (m, 2H), 1.5−1.8 (m, 3H), 1.34 (s, 9H), 1.25−1.5 (m, 2H), 0.85 (m, 6H). MS *m*/*z*: 602 $(M - H)^-$. HPLC homogeneity 97.7% (System A); 97.1% (System B).

***p*Tosyl-Glu(O*t*Bu)-Ala-LeuVSMe (22g).** ^{1}H NMR (400 MHz): δ 8.10 (d, J = 6.0 Hz, 1H), 7.98 (d, J = 6.8 Hz, 1H), 7.89 (d, J = 6.8 Hz, 1H), 7.62 (d, J = 8.0 Hz, 2H), 7.32 (d, J = 8.0 Hz, 2H), 6.60 (m, 2H), 4.51 (m, 1H), 3.97 (m, 1H), 3.73 (m, 1H), 2.99 (s, 3H), 2.36 (s, 3H), 2.11 (m, 2H), 1.5−1.8 (m, 3H), 1.36 (s, 9H), 1.2−1.45 (m, 2H), 1.08 (d, J = 6.8 Hz, 3H), 0.83 (m, 6H). MS *m*/*z*: 600 $(M - H)^-$. Anal. ($C_{27}H_{43}N_3O_8S_2$) C, H, N.

Compound 22h. ^{1}H NMR (400 MHz): δ 8.47 (d, J = 8.0 Hz, 1H), 8.11 (d, J = 7.2 Hz, 1H), 8.03 (d, J = 8.0 Hz, 1H), 7.24 (m, 10H), 6.64 (m, 2H), 5.10 (s, 1H), 4.52 (m, 1H), 4.29 (m, 1H), 4.19 (m, 1H), 2.99 (s, 3H), 2.14 (m, 2H), 1.83 (m, 1H), 1.50−1.75 (m, 2H), 1.36 (s, 9H), 1.3−1.5 (m, 2H), 1.21 (d, J = 7.2 Hz, 3H), 0.84 (m, 6H). MS *m*/*z*: 642 $(MH)^+$. Anal. ($C_{34}H_{47}N_3O_7S$) C, H, N.

Cbz-BocDab-Ser-LeuVSMe (22i). ^{1}H NMR (400 MHz): δ 8.02 (d, J = 8.4 Hz, 1H), 7.94 (d, J = 8.0 Hz, 1H), 7.54 (d, J = 7.2 Hz, 1H), 7.34 (m, 5H), 6.80 (broad t, J = 7.0 Hz, 1H), 6.69 (m, 2H), 5.07 (m, 1H), 5.02 (s, 2H), 4.57 (m, 1H), 4.27 (m, 1H), 4.04 (m, 1H), 3.60 (m, 2H), 2.99 (s, 5H), 1.77 (m, 1H), 1.61 (m, 2H), 1.36 (s, 9H), 1.2−1.5 (m, 2H), 0.86 (m, 6H). MS *m*/*z*: 611 $(M - H)^-$. Anal. ($C_{27}H_{41}N_3O_8S$) C, H, N.

Ac-Glu(OBn)-Ala-LeuVSMe (22j). ^{1}H NMR (400 MHz): δ 8.15 (d, J = 7.2 Hz, 1H), 8.09 (d, J = 8.0 Hz, 1H), 7.96 (d, J = 8.4 Hz, 1H), 7.37 (m, 5H), 6.68 (dd, J = 15.2, 4.4 Hz, 1H), 6.61 (d, J = 15.2 Hz, 1H), 5.08 (s, 2H), 4.53 (m, 1H), 4.24 (m, 2H), 2.99 (s, 3H), 2.40 (broad t, J = 7.6 Hz, 2H), 1.7−2.0 (m, 2H), 1.84 (s, 3H), 1.59 (m, 1H), 1.38 (m, 2H), 1.24 (d, J = 7.2 Hz, 3H), 0.85 (d, J = 6.8 Hz, 3H), 0.80 (d, J = 6.4 Hz, 3H). MS *m*/*z*: 524 $(MH)^+$. Anal. ($C_{25}H_{37}N_3O_7S$) C, H, N.

Compound 22k. ^{1}H NMR (400 MHz): δ 8.43 (d, J = 6.4 Hz, 1H), 8.12 (d, J = 8.8 Hz, 1H), 8.04 (d, J = 8.4 Hz, 1H), 7.51 (d, J = 8.0 Hz, 1H), 7.35 (m, 5H), 6.62 (s, 2H), 5.01 (ABq, 2H), 4.53 (m, 1H), 4.29 (q, J = 7.6 Hz, 1H), 4.13 (m, 1H), 4.08 (d, J = 8.8 Hz, 1H), 2.92 (s, 3H), 2.65 (d, J = 7.2 Hz, 2H), 1.64 (m, 1H), 1.3−1.6 (m, 2H), 1.39 (s, 9H), 1.26 (d, J = 6.8 Hz, 3H), 0.87 (m, 15H). MS *m*/*z*: 679 $(M - H)^-$. Anal. ($C_{33}H_{52}N_4O_9S\cdot0.5\ H_2O$) C, H, N.

Compound 22l. ^{1}H NMR (400 MHz): δ 8.04 (m, 3H), 7.50 (d, J = 7.6 Hz, 1H), 7.35 (m, 5H), 6.68 (dd, J = 15.2, 8.0 Hz, 1H), 6.62 (d, J = 15.2 Hz, 1H), 5.02 (m, 2H), 4.54 (m, 1H), 4.28 (m, 1H), 3.97 (m, 1H), 2.99 (s, 3H), 2.10 (m, 2H), 1.87 (m, 1H), 1.5−1.8 (m, 2H), 1.38 (m, 2H), 1.34 (s, 9H), 1.25 (m, 9H), 0.88 (d, J = 6.0 Hz, 3H), 0.82 (d, J = 6.0 Hz, 3H). MS *m*/*z*: 667 $(MH)^+$. Anal. ($C_{32}H_{50}N_4O_9S\cdot0.5\ H_2O$) C, H, N.

***p*Tosyl-NeopentylAsn-Ala-LeuVSMe (22m).** ^{1}H NMR (400 MHz): δ 8.43 (d, J = 6.4 Hz, 1H), 8.17 (d, J = 8.8 Hz, 1H), 8.12 (t, J = 6.0 Hz, 1H), 8.04 (d, J = 8.4 Hz, 1H), 7.65 (d, J = 8.6 Hz, 2H), 7.35 (d, J = 8.6 Hz, 2H), 6.59 (dd, J = 15.2, 4.0 Hz, 1H), 6.48 (d, J = 15.2 Hz, 1H), 4.48 (m, 1H), 4.00 (m, 1H), 3.52 (m, 1H), 2.88 (s, 3H), 2.6−2.9 (m, 3H), 2.44 (m, 1H), 2.37 (s, 3H), 1.57 (m, 2H), 1.38 (m, 1H), 1.06 (d, J = 7.6 Hz, 3H), 0.87 (d, J = 6.8 Hz, 3H), 0.82 (d, J = 7.2 Hz, 3H), 0.79 (s, 9H). MS *m*/*z*: 601 $(MH)^+$. Anal. ($C_{27}H_{44}N_4O_7S_2$) C, H, N.

***p*Tosyl-NeopentylAsn-Aib-LeuVSMe (22o).** ^{1}H NMR (400 MHz): δ 8.24 (s, 1H), 8.12 (m, 2H), 7.96 (d, J = 8.4 Hz, 1H), 7.68 (d, J = 8.4 Hz, 2H), 7.31 (d, J = 8.4 Hz, 2H), 6.62 (d, J = 15.2 Hz, 1H), 6.55 (dd, J = 15.2, 3.0 Hz, 1H), 4.41 (m, 1H), 4.02 (m, 1H), 2.86 (s, 3H), 2.6−2.9 (m, 3H), 2.46 (m, obscured by DMSO, 1H), 2.35 (s, 3H), 1.56 (m, 2H), 1.32 (m, 1H), 1.09 (s, 3H), 0.95 (s, 3H), 0.85 (d, J = 6.4 Hz, 3H), 0.78 (s, 12H). MS *m*/*z*: 613 $(M - H)^-$. Anal. ($C_{28}H_{46}N_4O_7S_2$) C, H, N.

1,3,4-Ketooxadiazole Syntheses. {1-[(*R*/*S*)-Hydroxy-(5-phenyl-[1,3,4]oxadiazol-2-yl)-(*S*)-methyl]-3-methylbutyl}-carbamic Acid *tert*-Butyl Ester (24). A solution of 2-phenyl-[1,3,4]oxadiazole (2.34 g, 16.0 mmol) in anhydrous THF (100 mL) was cooled with a dry ice bath and stirred under N_2. A solution of 1.6 M *n*-butyllithium in hexanes (10.0 mL, 16.0 mmol) was added. After

1 h, $MgBr_2$ diethyl etherate (4.13 g, 16.0 mmol) was added in one portion. After another 1 h, a solution of freshly prepared Boc leucinal (1.94 g, 8.0 mmol)[38] was added as a solution in 20 mL of THF. After an additional 1.5 h at low temperature, 1 M HCl was added, and the cold bath was removed. The mixture was allowed to warm and then was transferred to a sep funnel. Ether (100 mL) was added. The organic phase was separated, and the aqueous phase was extracted twice more with ether. The combined organic phase was washed with water, aq $NaHCO_3$, and brine and then dried over $MgSO_4$. Filtration and solvent evaporation gave an oily residue that was flash chromatographed on silica gel, eluting with a 25−50% EtOAc/hexane gradient, to give **24** (4.27 g, 70% yield). ^{1}H NMR (400 MHz): δ 7.94 (d, J = 6.0 Hz, 2H), 7.58 (s, 3H), 6.75, 6.64 (2d, J = 9.2, 8.8 Hz, 1H total), 6.30, 6.10 (2d, J = 6.0 Hz, 1H total), 4.85, 4.52 (2m, 1H total), 3.85 (m, 1H), 1.1−1.7 (m, 12H), 0.86 (m, 6H). MS *m*/*z*: 384 $(M + Na)^+$.

2-(*S*)-Amino-4-methyl-1-(5-phenyl-[1,3,4]oxadiazol-2-yl)-(*R*/*S*)-pentan-1-ol Hydrochloride (25). Compound **24** (11.9 g, 32.9 mmol) was dissolved in 25 mL of CH_2Cl_2. A 4 M solution of HCl in 1,4-dioxane (100 mL, 400 mmol) was added with stirring. After 2 h, ether (400 mL) was added, which caused an oil to form. The supernatant was decanted, and the oil was triturated with more ether to afford **25** as a pale yellow solid (9.73 g, >99% yield). ^{1}H NMR (400 MHz): δ 8.00 (m, 2H), 7.62 (m, 3H), 4.57 (m, 1H), 4.12 (broad s, 1H), 3.06 (m, 1H), 1.80 (m, 1H), 1.0−1.5 (m, 2H), 0.87 (m, 6H). MS *m*/*z*: 262 $(MH)^+$.

(1-{1(*R*/*S*)-[Hydroxy-(5-phenyl-[1,3,4]oxadiazol-2-yl)-(*S*)-methyl]-3-methyl-butylcarbamoyl}-2-(*S*)-methoxyethyl)-carbamic Acid *tert*-Butyl Ester (26). *N*-α-Boc-*O*-methyl-L-serine (2.19 g, 10.0 mmol), HOBT (1.62 g, 12.0 mmol), EDC (2.01 g, 10.5 mmol), and NMM (1.4 mL, 12.5 mmol) were stirred in anhyd CH_2Cl_2 (150 mL). After 5 min, compound **25** (2.61 g, 10.0 mmol) dissolved in CH_2Cl_2 (50 mL), and more NMM (1.4 mL, 12.5 mmol) was added. After 3 h, the reaction mixture was transferred to a sep funnel and washed twice with 100 mL portions of 0.5 M HCl. The organic phase was separated, washed once with water (50 mL) and twice with saturated $NaHCO_3$ (100 mL). The organic phase was dried over $MgSO_4$. Filtration and solvent evaporation gave a tan foam. This was flash chromatographed on silica gel with 5% MeOH in CH_2Cl_2 to give **26** as a brittle, pale yellow foam, (3.65 g, 79%), a mixture of diastereomers. ^{1}H NMR (400 MHz): δ 7.96 (m, 2H), 7.82, 7.72 (2d, J = 9.6, 8.4 Hz, 1H), 7.60 (m, 5H), 6.85, 6.73 (2d, J = 8.4, 7.6 Hz, 1H), 6.33, 6.28 (2d, J = 6.0, 4.8 Hz, 1H), 4.90, 4.64 (2 broad t, J = 4.4, 7.6 Hz, 1H), 4.15−4.35 (m, 1H), 4.09, 3.93 (2m, 1H), 3.10, 2.96 (2s, 3H), 1.3−1.7 (m, 3H), 1.35, 1.34 (2s, 9H), 0.88 (d, J = 6.8 Hz, 3H), 0.83 (d, J = 6.0 Hz, 3H). gCOSY shows coupling between δ 6.33 (O*H* of diastereomer 1) and δ 4.64 (C*H*OH of diastereomer 1) peaks, and between δ 6.28 (O*H* of diastereomer 2) and δ 4.90 (C*H*OH of diastereomer 2) peaks. MS *m*/*z*: 485 $(M + Na)^+$.

2-(*S*)-Amino-*N*-{1(*R*/*S*)-[hydroxy-(5-phenyl-[1,3,4]oxadiazol-2-yl)-(*S*)-methyl]-3-methylbutyl}-3-methoxy-propionamide Hydrochloride (27). Compound **26** (3.55 g, 7.68 mmol) was dissolved in 4 M HCl (36 mL, 144 mmol) in 1,4-dioxane. After 2 h, the volatiles were removed by rotary evaporation, and the residue was triturated with ether (15 mL). Filtration and drying gave compound **27** as a beige solid (3.06 g, >99%), a mixture of diastereomers. ^{1}H NMR (400 MHz): δ 8.51 (d, J = 8.8 Hz, 1H), 7.98 (m, 3H), 7.62 (m, 5H), 4.97, 4.66 (2d, J = 2.0, 8.4 Hz, 1H), 4.31 (m, 1H), 3.95, 3.87 (2m, 1H), 3.2−3.8 (m, 2H), 3.12, 3.07 (2s, 3H), 1.66 (m, 1H), 1.51 (m, 2H), 0.90 (t, J = 6.8 Hz, 6H). MS *m*/*z*: 363 $(MH)^+$.

***N*4-(2,2-Dimethylpropyl)-*N*1-(1-{1(*R*/*S*)-[hydroxy-(5-phenyl-[1,3,4]oxadiazol-2-yl)-(*S*)-methyl]-3(*S*)-methylbutylcarbamoyl}-2-methoxyethyl)-2(*S*)-(toluene-4-sulfonylamino)-succinamide (28d).** Compound **21** (2.68 g, 7.52 mmol) and HOBT (3.00 g, 7.52 mmol) were stirred in CH_2Cl_2 (130 mL). EDC (1.51 g, 7.90 mmol) and *N*-methylmorpholine (1.65 g, 15.0 mmol) were added. After 8 min, compound **27** (3.00 g, 7.52 mmol) and more NMM (1.65 g, 15.0 mmol) were added. After 2.5 h, the reaction mixture was transferred to a sep funnel and washed thrice with 0.5 M HCl. The organic phase was washed with water, sat. $NaHCO_3$, and brine. Drying over anhyd $MgSO_4$ followed by filtration and solvent evaporation gave a sticky brown oil. Trituration with ether followed by filtration and drying of the precipitate gave compound **28d** (1.93 g, 37% yield) as a crude mixture of diastereomers that was used directly in the next step. Mp 109−112 °C. ^{1}H NMR (400 MHz): δ 7.65−8.1 (m, 7H), 7.57 (m, 4H), 7.26 (m, 2H), 6.27, 6.06 (2d, exchange with D_2O, J = 6.4 Hz, 1H), 4.84, 4.59 (2t, J = 6.4 Hz, 1H), 3.9−4.3 (m, 3H), 2.9−3.4 (m, 2H), 3.11, 2.99 (2s, 3H), 2.71 (m, 2H), 2.3−2.5 (m, 2H), 2.35, 2.31 (2s, 3H), 1.3−1.7 (m, 3H), 0.75−0.9 (m, 6H), 0.80, 0.77 (2s, 9H). MS *m*/*z*: 702 $(MH)^+$.

***p*Ts-NeopentylAsn-Ser(OMe)-LeuKODPh (29d).** Compound **28d** (2.20 g, 3.14 mmol) was dissolved in 50 mL of water-saturated CH_2Cl_2 and was vigorously stirred. Dess−Martin periodinane (2.00 g, 4.71 mmol) was added in one portion. After 2 h, more Dess−Martin periodinane (0.67 g, 1.57 mmol) was added. After 4 h, a solution of 0.26 M $Na_2S_2O_3$ in sat. $NaHCO_3$ (300 mL) was added with vigorous stirring. After 30 min, the mixture was transferred to a sep funnel, and CH_2Cl_2 (50 mL) was added. The organic phase was separated and washed twice with the previously described quenching solution and then once with sat. $NaHCO_3$, water, and brine. Drying over anhydrous $MgSO_4$ followed by filtration and solvent evaporation afforded 1.93 g of a pale yellow solid. Flash chromatography on silica gel with 2.5/5.0/92.5 MeOH/acetone/CH_2Cl_2 gave **29d** (1.73 g, 79%) as a pale yellow solid; mp 161−163 °C. ^{1}H NMR (400 MHz): δ 8.56 (d, J = 6.4 Hz, 1H), 8.16 (d, J = 7.6 Hz, 1H), 8.06 (d, J = 8.0 Hz, 2H), 7.92 (d, J = 8.8 Hz, 1H), 7.77 (t, J = 6 Hz, 1H), 7.65 (m, 5H), 7.29 (d, J = 8.0 Hz, 2H), 5.13 (m, 1H), 4.15 (m, 2H), 3.42 (m, 1H), 3.25 (m, 1H), 3.13 (s, 3H), 2.79 (m, 2H), 2.35 (s, 3H), 2.31 (m, 2H), 1.71 (m, 3H), 0.93 (broad s, 6H), 0.78 (s, 9H). MS *m*/*z*: 699.6 $(MH)^+$. Anal. ($C_{34}H_{46}N_6O_8S$) C, H, N.

Other Compounds Prepared by This General Method. Ms-NeopentylAsn-Ala-LeuKODPh (29a). ^{1}H NMR (400 MHz): δ 8.52 (d, J = 6.4 Hz, 1H), 8.26 (d, J = 7.2 Hz, 1H), 8.07 (d, J = 7.2 Hz, 2H), 7.85 (broad t, J = 6.0 Hz, 1H), 7.67 (m, 3H), 7.41 (d, J = 8.4 Hz, 1H), 5.16 (m, 1H), 4.29 (m, 1H), 4.14 (m, 1H), 2.75−2.95 (m, 2H), 2.86 (s, 3H), 2.55 (m, obscured by DMSO, 2H), 1.6−1.9 (m, 3H), 1.20 (d, J = 7.2 Hz, 3H), 0.95 (d, J = 6.0 Hz, 6H), 0.82 (s, 9H). MS *m*/*z*: 615.5 $(M + Na)^+$. Anal. ($C_{27}H_{40}N_6O_7S$) C, H, N.

***m*Ts-NeopentylAsn-Ala-LeuKODPh (29b).** ^{1}H NMR (400 MHz): δ 8.44 (d, J = 6.4 Hz, 1H), 8.15 (d, J = 7.6 Hz, 1H), 8.06 (d, J = 7.6 Hz, 2H), 8.00 (d, J = 9.2 Hz, 1H), 7.82 (t, J = 6.0 Hz, 1H), 7.65 (m, 3H), 7.54 (m, 2H), 7.38 (m, 2H), 5.13 (m, 1H), 4.08 (m, 1H), 3.94 (m, 1H), 2.81 (m, 2H), 2.3−2.6 (m, overlaps with DMSO, 2H), 2.34 (s, 3H), 1.70 (m, 3H), 1.00 (d, J = 7.2 Hz, 3H), 0.93 (m, 6H), 0.80 (s, 9H). gCOSY shows coupling between δ 1.00 (Ala CH_3) and δ 3.94(Ala C*H*) and between δ 2.81 (HNCH_2*t*-Bu) and δ 7.82 (*H*NCH_2*t*-Bu). MS *m*/*z*: 691 $(M + Na)^+$. Anal. ($C_{33}H_{44}N_6O_7S$) C, H, N.

***p*Ts-NeopentylAsn-Ala-LeuKODPh (29c).** ^{1}H NMR (400 MHz): δ 8.43 (d, J = 6.0 Hz, 1H), 8.12 (d, J = 6.8 Hz, 1H), 8.05 (d, J = 7.6 Hz, 2H), 7.95 (d, J = 8.8 Hz, 1H), 7.80 (broad t, J = 6.0 Hz, 1H), 7.62 (m, 5H), 7.28 (d, J = 7.6 Hz, 2H), 5.11 (m, 1H), 4.02 (m, 1H), 3.92 (m, 1H), 2.80 (m, 2H), 2.51 (m, overlaps with DMSO, 2H), 2.34 (s, 3H), 1.69 (m, 3H), 1.00 (d, J = 7.2 Hz, 3H), 0.93 (broad s, 6H), 0.79 (s, 9H). MS *m*/*z*: 667 $(M - H)^-$. Anal. ($C_{33}H_{44}N_6O_7S\cdot0.5\ H_2O$) C, H, N.

***p*Ts-NeopentylAsn-Ala-AibKODPh (29e).** ^{1}H NMR (400 MHz): δ 8.78 (s, 1H), 8.12 (d, J = 6.8 Hz, 1H), 8.04 (d, J = 7.6 Hz, 2H), 7.90 (broad s, 1H), 7.84 (broad t, J = 6.0 Hz, 1H), 7.62 (m, 5H), 7.27 (d, J = 7.6 Hz, 2H), 4.01 (m, 1H), 3.67 (m, 1H), 2.82 (d, J = 6.0 Hz, 2H), 2.3−2.6 (m, overlaps with DMSO, 2H), 2.32 (s, 3H), 1.54 (s, 3H), 1.43 (s, 3H), 0.80 (s, 12H). gCOSY shows coupling between peaks at δ 0.90 (Ala CH_3) and δ 3.67 (Ala C*H*), between δ 2.40 (CHCH_2CO) and δ 4.01 (C*H*CH_2CO), and between δ 7.84 (*t*-BuCH_2N*H*) and δ 2.82 (*t*-BuCH_2NH). MS *m*/*z*: 639 $(M - H)^-$. HPLC homogeneity 98.6% (System A); 100% (System B).

Compound 29f. ^{1}H NMR (400 MHz): δ 8.45 (d, J = 6.0 Hz, 1H), 8.18 (d, J = 7.6 Hz, 1H), 7.80 (broad t, J = 5.2 Hz, 1H), 7.36

(d, $J = 9.2$ Hz, 1H), 5.08 (m, 1H), 4.27 (m, 1H), 4.03 (m, 1H), 3.29 (m, obscured by HOD, 1H), 2.85 (d, $J = 6.0$ Hz, 2H), 2.60 (s, 6H), 2.4−2.7 (m, overlaps with DMSO, 2H), 1.74 (m, 1H), 1.62 (m, 2H), 1.32 (dd, $J = 6.8$, 1.2 Hz, 6H), 1.17 (d, $J = 7.2$ Hz, 3H), 0.90 (m, 6H), 0.81 (s, 9H). MS *m*/*z*: 587 $(M - H)^-$. Anal. Calcd for $C_{25}H_{45}N_7O_7S$: C, 51.09; H, 7.72; N, 16.68. Found: C, 51.10; H, 7.47; N, 16.11.

Compound 29g. ^{1}H NMR (400 MHz): δ 8.36 (d, $J = 6.0$ Hz, 1H), 8.08 (d, $J = 7.6$ Hz, 1H), 7.93 (d, $J = 8.4$ Hz, 1H), 7.82 (d, $J = 7.2$ Hz, 2H), 7.76 (broad t, $J = 5.6$ Hz, 1H), 7.60 (d, $J = 7.2$ Hz, 2H), 7.28 (d, $J = 8.0$ Hz, 2H), 6.83 (d, $J = 8.0$ Hz, 2H), 5.10 (m, 1H), 4.04 (m, 1H), 3.94 (m, 1H), 3.02 (s, 6H), 2.79 (m, 2H), 2.3−2.55 (m, obscured by DMSO, 2H), 2.33 (s, 3H), 1.5−1.9 (m, 3H), 0.99 (d, $J = 7.2$ Hz, 3H), 0.92 (m, 6H), 0.78 (s, 9H). MS *m*/*z*: 710.5 $(M - H)^-$. Anal. ($C_{35}H_{49}N_7O_7S \cdot 0.5\ H_2O$) C, H, N.

Compound 29h. ^{1}H NMR (400 MHz): δ 8.49 (d, $J = 6.8$ Hz, 1H), 8.14 (d, $J = 8.0$ Hz, 1H), 7.92 (d, $J = 9.2$ Hz, 1H), 7.83 (d, $J = 7.6$ Hz, 2H), 7.75 (broad t, $J = 6.0$ Hz, 1H), 7.61 (d, $J = 7.6$ Hz, 2H), 7.28 (d, $J = 7.6$ Hz, 2H), 6.83 (d, $J = 7.6$ Hz, 2H), 5.11 (m, 1H), 4.16 (m, 2H), 3.40 (m, 1H), 3.31 (s, 3H), 3.24 (m, 1H), 3.03 (s, 6H), 2.78 (d, $J = 6.0$ Hz, 2H), 2.25−2.55 (m, obscured by DMSO, 2H), 2.32 (s, 3H), 1.6 − 1.8 (m, 3H), 0.90 (m, 6H), 0.78 (s, 9H). MS *m*/*z*: 741 $(M - H)^-$. Anal. ($C_{36}H_{51}N_7O_8S \cdot 0.5\ H_2O$) C, H, N.

Compound 29i. ^{1}H NMR (400 MHz): δ 8.53 (d, $J = 6.4$ Hz, 1H), 8.21 (d, $J = 7.2$ Hz, 1H), 8.07 (dd, $J = 7.2$, 1.2 Hz, 2H), 8.02 (d, $J = 7.6$, 1.2 Hz, 1H), 7.62 (m, 5H), 7.27 (m, 5H), 7.18 (d, $J = 7.2$ Hz, 2H), 5.13 (m, 1H), 4.34 (m, 1H), 4.31 (s, 2H), 4.10 (m, 1H), 3.38 (m, 2H), 3.31 (s, 3H), 3.25 (d, $J = 6.0$ Hz, 2H), 2.32 (s, 3H), 1.69 (m, 2H), 1.55 (m, 1H), 0.89 (m, 6H). MS *m*/*z*: 692 $(MH)^+$. Anal. Calcd for $C_{35}H_{41}N_5O_8S \cdot H_2O$: C, 59.22; H, 6.11; N, 9.87. Found: C, 59.05; H, 5.59; N, 9.83.

Compound 29j. ^{1}H NMR (400 MHz): δ 8.47 (d, $J = 6.4$ Hz, 1H), 8.13 (d, $J = 7.6$ Hz, 1H), 8.06 (d, $J = 6.4$ Hz, 2H), 7.98 (d, $J = 8.8$ Hz, 1H), 7.62 (m, 5H), 7.24 (d, $J = 8.0$ Hz, 2H), 7.11 (m, 4H), 5.12 (m, 1H), 4.30 (s, 2H), 4.16 (m, 1H), 4.03 (m, 1H), 3.41 (m, 2H), 2.33 (s, 3H), 2.14 (s, 3H), 1.70 (m, 2H), 1.53 (m, 1H), 1.02 (d, $J = 7.2$ Hz, 3H), 0.91 (m, 6H). MS *m*/*z*: 699 $(M + Na)^+$. Anal. ($C_{35}H_{41}N_5O_7S \cdot 0.5\ H_2O$) C, H, N.

Compound 29k. ^{1}H NMR (400 MHz): δ 8.45 (d, $J = 6.8$ Hz, 1H), 8.14 (d, $J = 7.2$ Hz, 1H), 8.04 (m, 3H), 7.61 (m, 5H), 7.26 (m, 5H), 7.13 (m, 1H), 5.13 (m, 1H), 4.32 (s, 2H), 4.16 (m, 1H), 4.02 (m, 1H), 3.39 (d, $J = 6.4$ Hz, 2H), 2.31 (s, 3H), 1.70 (m, 2H), 1.53 (m, 1H), 1.05 (d, $J = 7.2$ Hz, 3H), 0.90 (m, 6H). MS *m*/*z*: 718.3 $(M + Na)^+$. Anal. ($C_{34}H_{38}ClN_5O_7S \cdot 0.5\ H_2O$) C, H, N.

Compound 29l. ^{1}H NMR (400 MHz, $CDCl_3$): δ 8.15 (d, $J = 6.8$ Hz, 2H), 7.71 (d, $J = 8.4$ Hz, 2H), 7.59 (m, 1H), 7.54 (m, 2H), 7.27 (m, 3H), 7.13 (m, 4H), 7.07 (d, $J = 8$ Hz, 1H), 5.54 (m, 1H), 5.13 (m, 1H), 4.50 (m, 1H), 4.33 (ABq, 2H), 3.77 (m, 2H), 3.44 (m, 1H), 2.44 (s, 3H), 2.36 (s, 3H), 1.6−2.0 (m, 3H), 1.37 (d, $J = 7.2$ Hz, 3H), 1.04 (d, $J = 6.4$ Hz, 3H), 0.99 (d, $J = 6.0$ Hz, 3H). MS *m*/*z*: 699 $(M + Na)^+$. Anal. ($C_{35}H_{41}N_5O_7S$) C, H, N.

In Vitro 20S Proteasome Inhibition Assays. Human 20S proteasome was obtained from Affiniti Research Products Ltd., Mamhead, Exeter, U.K. The three distinct proteolytic activities of the 20S proteaseome were measured by monitoring the hydrolysis of an optimized peptidal 7-amino-4-methyl coumarin substrate for either the chymotryptic, tryptic or post glutamyl-peptide hydrolyzing activity (PGPH Activity) of the enzyme. Hydrolysis of the given substrate was measured using an fMax plate reader (Molecular Devices, Sunnyvale, CA) at ambient temperature with a 355 ± 38 nm excitation filter and a 460 ± 25 nm emission filter. The velocity of the enzyme-catalyzed reaction was obtained from the linear portion of the progress curves (usually the first 10 min after the addition of substrate). Apparent inhibition constants, $K_{i_{app}}$s, were calculated for reversible inhibitors from the reaction velocity data generated at the various inhibitor concentrations using the software package, BatchKi (Biokin Ltd., Pullman, WA). BatchKi provides a parametric method for the determination of inhibitor potency using a transformation of the tight binding inhibition model described by Morrison[39,40] and further refines the $K_{i_{app}}$ values by nonlinear least-squares regression. For reversible, competitive inhibitors, the apparent inhibition constant, $K_{i_{app}}$, is related to the true thermodynamic binding constant, K_i, by the following relationship: $K_i = K_{i_{app}}/(1 + [\text{Substrate}]/K_m)$. Because, except for trypsin-like proteasome activity, substrates are supplied in the assays at their K_m, $K_i = K_{i_{app}}/2$.

Assaying the Chymotryptic Activity of the 20S Proteasome. Human 20S proteasome was incubated at a final concentration of 2 nM with test compound present at variable concentrations. The reaction buffer consisted of 50 mM Tris (pH 7.4), 50 mM NaCl, 0.5 mM EDTA, 0.05% Tween-20, 0.035% SDS, and 5% DMSO. After 60 min of enzyme and inhibitor incubation, the reactions were initiated with the addition of the substrate, Suc-Leu-Leu-Val-Tyr-AMC (Bachem Bioscience Inc., King of Prussia, PA). The final concentration of substrate in the reaction was 50 μM.

Assaying the Tryptic Activity of the 20S Proteasome. Human 20S proteasome was incubated at a final concentration of 20 nM with test compound present at variable concentrations. The reaction buffer consisted of 50 mM Tris (pH 7.4), 50 mM NaCl, 0.5 mM EDTA, 0.05% Tween-20, 0.035% SDS, and 5% DMSO. After 60 min of enzyme and inhibitor incubation, the reactions were initiated with the addition of the substrate, Boc-Leu-Arg-Arg-AMC (Bachem Bioscience Inc., King of Prussia, PA). The final concentration of substrate in the reaction was 85 μM.

Assaying the Post Glutamyl-Peptide Hydrolyzing Activity of the 20S Proteasome. Human 20S proteasome was incubated at a final concentration of 10 nM with the test compound present at variable concentrations. The reaction buffer consisted of 50 mM Tris (pH 7.4), 50 mM NaCl, 0.5 mM EDTA, 0.05% Tween-20, 0.035% SDS, and 5% DMSO. After 60 min of enzyme and inhibitor incubation, the reactions were initiated with the addition of the substrate, Z-Leu-Leu-Glu-AMC (California Peptide Research, Inc., Napa, CA). The final concentration of the substrate in the reaction was 80 μM.

Determination of the Reversibility of 20S Proteasome Inhibition. The reversibility of 20S proteasome inhibition by **29c** was carried out by preforming the enzyme−inhibitor complex during a 60 min incubation phase. Compound **29c** was supplied at 150 nM during the incubation phase along with the 150 nM active sites of the 20S proteasome. Following incubation, the reaction was diluted 50-fold into an assay buffer containing 50 μM substrate such that the final concentration of **29c** and enzyme was 3.0 nM. The recovery of chymotryptic activity of the 20S proteasome was monitored as described above as a function of time. The kinetic parameters for the first order recovery of enzyme activity were obtained by standard methods. Control reactions were performed in parallel in which the inhibitor was omitted from the initial incubation phase of the experiment to obtain the uninhibited rate. Additionally, control assays were performed to demonstrate that the enzyme was fully inhibited during the incubation phase.

Assays for Cathepsin B and Cathepsin S Inhibition. Inhibition of cathepsin B and cathepsin S was determined using the methods previously described.[26]

Determination of Compound Solubility. Kinetic solubility was determined in PBS at pH 7.4, containing 5% DMSO. The samples were prepared by adding 10 μL of 10 mM DMSO stock to 190 μL of PBS. After vortexing, the samples were centrifuged at 4300 rpm for 10 min to precipitate any insoluble materials. The supernatant was then analyzed by HPLC with UV detector and quantified against a calibration standard.

Plasma Stability Assessment. Human plasma stability was determined by incubating compound at 5 μg/mL in human plasma. The samples were incubated at 37 °C for 120 min. The disappearance of the parent compound was monitored by LC/MS/MS. The percentage remaining of the parent compound was calculated on the basis of the peak area of the parent compound at the end of incubation to that obtained at 0 min.

Cell Growth Inhibition Assay. The human prostate tumor cell line PC3 was obtained from the American Type Tissue Culture Collection (ATCC). The effect of proteasome inhibitors on human PC3 cell growth inhibition was monitored in an alamarBlue

fluorometric assay as described by de Fries and Mitsuhashi.[36] Briefly, 5000 cells/well were plated in 96-well plates in complete media. The compounds were assayed in triplicate wells at eight concentrations from 0.005 to 20 μM, except for epoxomicin, which was tested at six concentrations from 0.0036 to 360 nM. Each well contained 0.2% DMSO. The cells were exposed to compounds for two doubling times (44 h). At 44 h, the alamarBlue reagent was added to cells, and the plates were incubated for 4 h at 37 °C. At 48 h, the fluorescence was determined using the plate reader, and the IC_{50} values were calculated for each compound. The concentration required to inhibit cell growth by 50% (IC_{50}) was determined by two point linear interpolation.

Acknowledgment. We express our gratitude to Mimi Li, Jeremy Parr, and Joanne Fanucchi for their expert help in compound purification, compound analysis, and manuscript preparation, respectively.

Supporting Information Available: Elemental analyses for the products synthesized. The material is available free of charge via the Internet at http://pubs.acs.org.

References

(1) (a) Goldberg, A. L. Protein degradation and protection against misfolded or damaged proteins. *Nature* **2003**, *426*, 895−899. (b) Wojcik, C. Ubiquitin- and proteasome-dependent pathway of protein degradation as an emerging therapeutic target. *Emerging Ther. Targets* **2000**, *4*, 89−111. (c) Rock, K. L.; Gramm, C.; Rothstein, L.; Clark, K.; Stein, R.; Dick, L.; Hwang, D.; Goldberg, A. L. Inhibitors of the proteasome block the degradation of most cell proteins and the generation of peptides presented on MHC class I molecules. *Cell* **1994**, *78*, 761−771. (d) Kessler, B.; Hong, X.; Petrovic, J.; Borodovsky, A.; Dantuma, N. P.; Bogyo, M.; Overkleeft, H. S.; Ploegh, H.; Glas, R. Pathways accessory to proteasomal proteolysis are less efficient in major histocompatibility complex class I antigen production. *J. Biol. Chem.* **2003**, *278*, 10013−10021.

(2) (a) Voges, D.; Zwickl, P.; Baumeister, W. The 26S Proteasome: A molecular machine designed for controlled proteolysis. *Annu. Rev. Biochem.* **1999**, *68*, 1015−1068. (b) Bochtler, M.; Ditzel, L.; Groll, M.; Hartmann, C.; Huber, R. The proteasome. *Annu. Rev. Biophys. Biomol. Struct.* **1999**, *28*, 295−317.

(3) Walz, J.; Erdmann, A.; Kania, M.; Typke, D.; Koster, A. J.; Baumeister, W. 26S Proteasome structure revealed by three-dimensional electron microscopy. *J. Struct. Biol.* **1998**, *121*, 19−29.

(4) (a) Groll, M.; Ditzel, L.; Lowe, J.; Stock, D.; Bochtler, M.; Bartunik, H. D.; Huber, R. Structure of 20S proteasome from yeast at 2.4Å resolution. *Nature* **1997**, *386*, 463−471. (b) Unno, M.; Mizushima, T.; Morimoto, Y.; Tomisugi, Y.; Tanaka, K.; Yasuoka, N.; Tsukihara, T. The structure of the mammalian 20S proteasome at 2.75Å resolution. *Structure* **2002**, *10*, 609−618.

(5) (a) Dick, T. P.; Nussbaum, A. K.; Deeg, M.; Heinemeyer, W.; Groll, M.; Schirle, M.; Keilholz, W.; Stevanovic, S.; Wolf, D. H.; Huber, R.; Rammensee, H.-G.; Schild, H. Contribution of proteasomal β-subunits to the cleavage of peptide substrates analyzed with yeast mutants. *J. Biol. Chem.* **1998**, *273*, 25637−25646. (b) Jager, S.; Groll, M.; Huber, R.; Wolf, D. H.; Henimeyer, W. Proteasome β-type subunits: Unequal roles of propeptides in core particle maturation and a hierarchy of active site functions. *J. Mol. Biol.* **1999**, *291*, 997−1013.

(6) Palombella, V. J.; Rando, O. J.; Goldberg, A. L.; Maniatis, T. The ubiquitin-proteasome pathway is required for processing the NF-κB1 precursor protein and the activation of NF-κB1. *Cell* **1994**, *78*, 773−785.

(7) (a) Adams, J.; Palombella, V. J.; Elliott, P. J.; Proteasome inhibition: a new strategy in cancer treatment. *Invest. New Drugs* **2000**, *18*, 109−121. (b) Almond, J. B.; Cohen, G. M.; The proteasome: a novel target for cancer chemotherapy. *Leukemia* **2002**, *16*, 433−443.

(8) Adams, J.; Kauffman, M. Development of the proteasome inhibitor Velcade (Bortezomib). *Cancer Invest.* **2004**, *22*, 304−311.

(9) Schubert, U.; Ott, D. E.; Chertova, E. N.; Welker, R.; Tessmer, U.; Princiotta, M. F.; Bennink, J. R.; Krausslich, H.-G.; Yewdell, J. W. Proteasome inhibition interferes with Gag polyprotein processing, release, and maturation of HIV-1 and HIV-2. *Proc. Natl. Acad. Sci. U.S.A.* **2000**, *97*, 13057−13062.

(10) (a) Piccinini, M.; Rinaudo, M. T.; Chiapello, N.; Ricotti, E.; Baldovino, S.; Mostert, M.; Tovo, P.-A. The human 26S proteasome is a target of antiretroviral agents. *AIDS* **2002**, *16*, 693−700. (b) Pajonk, F.; Himmelsbach, J.; Riess, K.; Sommer, A.; McBride, W. H.; The human immunodeficiency virus (HIV)-1 protease inhibitor Saquinavir inhibits proteasome function and causes apoptosis and radiosensitization in non-HIV-associated human cancer cells. *Cancer Res.* **2002**, *62*, 5230−5235. (c) Andre, P.; Groettrup, M.; Klenerman, P.; De Giuli, R.; Booth, B. L.; Cerundolo, V.; Bonneville, M.; Jotereau, F.; Zinkernagel, R. M.; Lotteau, V. An inhibitor of HIV-1 protease modulates proteasome activity, antigen presentation, and T cell responses. *Proc. Natl. Acad. Sci. U.S.A.* **1998**, *95*, 13120−13124. (d) Schmidtke, G.; Holhutter, H.-G.; Bogyo, M.; Kairies, N.; Groll, M.; de Giuli, R.; Emch, S.; Groettrup, M. How an inhibitor of the HIV-1 protease modulates proteasome activity. *J. Biol. Chem.* **1999**, *274*, 35734−35740.

(11) Kalogeris, T.; Gray, L.; Laroux, F. S.; Cockrell, A.; Fuseler, J.; Conner, E. M.; Brand, S.; Grisham, M. B. Selective proteasome inhibitors as anti-inflammatory agents. *Expert Opin. Invest. Drugs* **1999**, *8*, 1397−1407.

(12) Di Napoli, M.; McLaughlin, B. The ubiquitin-proteasome system as a drug target in cerebrovascular disease: Therapeutic potential of proteasome inhibitors. *Curr. Opin. Invest. Drugs* **2005**, *6*, 686−699.

(13) Nazif, T.; Bogyo, M. Global analysis of proteasomal substrate specificity using positional-scanning libraries of covalent inhibitors. *Proc. Natl. Acad. Sci. U.S.A.* **2001**, *98*, 2967−2972.

(14) Kisselev, A. F.; Garcia-Calvo, M.; Overkleeft, H. S.; Peterson, E.; Pennington, M. W.; Ploegh, H. L.; Thornberry, N. A.; Goldberg, A. L. The caspase-like sites of proteasomes, their substrate specificity, new inhibitors and substrates, and allosteric interactions with the trypsin-like sites. *J. Biol. Chem.* **2003**, *278*, 35869−35877.

(15) Elofsson, M.; Splittgerber, U.; Myung, J.; Mohan, R.; Crews, C. M. Toward subunit-specific proteasome inhibitors: synthesis and evaluation of peptide α',β'-epoxyketones. *Chem. Biol.* **1999**, *6*, 811−822.

(16) Myung, J.; Kim, K. B.; Lindsten, K.; Dantuma, N. P.; Crews, C. M. Lack of proteasome active site allostery as revealed by subunit-specific inhibitors. *Mol. Cell* **2001**, *7*, 411−420.

(17) The following nonstandard abbreviations have been used in this paper: Aib, 2-aminoisobutyric acid; CatB, cathepsin B; CatS, cathepsin S; Dab, (*S*)-2,4-diaminobutyric acid; DMS, dimethylsulfamoyl; hGln, (*S*)-homoglutamine; hGlu, (*S*)-homoglutamic acid; hPhe, (*S*)-homophenylalanine; IBCF, isobutylchloroformate; KOD, 2-keto-1,3,4-oxadiazole; VS, vinyl sulfone.

(18) Bogyo, M.; McMaster, J. S.; Gaczynska, M.; Tortorella, D.; Goldberg, A. L.; Ploegh, H. Covalent modification of the active site threonine of proteasomal β subunits and the *Escherichia* coli homolog HslV by a new class of inhibitors. *Proc. Natl. Acad. Sci. U.S.A.* **1997**, *94*, 6629−6634.

(19) Eberlein, W.; Heider, J.; Machleidt, H. Steroidal cariotonics. II. Replacement of the butenolide ring of cardiac glycosides by unbranched open chain π-electron systems. *Chem. Ber.* **1974**, *107*, 1275−1284.

(20) Ohmoto, K.; Yamamoto, T.; Okuma, M.; Horiuchi, T.; Imanishi, H.; Odagaki, Y.; Kawabata, K.; Sekioka, T.; Hirota, Y.; Matsuoka, S.; Nakai, H.; Toda, M. Development of orally active nonpeptidic inhibitors of human neutrophil elastase. *J. Med. Chem.* **2001**, *44*, 1268−1285.

(21) Copeland, R. A. *Evaluation of Enzyme Inhibitors in Drug Discovery*; John Wiley & Sons: Hoboken, NJ, 2005; pp 214−249.

(22) Groll, M.; Heinemeyer, W.; Jager, S.; Ullrich, T.; Bochtler, M.; Wolf, D. H.; Huber, R. The catalytic sites of 20S proteasomes and their role in subunit maturation: A mutational crystallographic study. *Proc. Natl. Acad. Sci. U.S.A.* **1999**, *96*, 10976−10983.

(23) (a) Chen, P.; Hochstrasser, M. Autocatalytic subunit processing couples active site formation in the 20S proteasome to completion of assembly. *Cell* **1996**, *86*, 961−972. (b) Arendt, C. S.; Hochstrasser, M. Identification of the yeast 20S proteasome catalytic centers and subunit interactions required for active-site formation. *Proc. Natl. Acad. Sci. U.S.A.* **1997**, *94*, 7156−7161.

(24) (a) Palmer, J. T.; Rasnick, D.; Klaus, J. L.; Bromme, D. Vinyl sulfones as mechanism-based cysteine protease inhibitors. *J. Med. Chem.* **1995**, *38*, 3193−3196. (b) Bromme, D.; Klaus, J. L.; Okamoto, K.; Rasnick, D.; Palmer, J. T. Peptidyl vinyl sulfones: a new class of potent and selective cysteine protease inhibitors. *Biochem. J.* **1996**, *315*, 85−89.

(25) Kirschke, H.; Barrett, A. J.; Rawlings, N. D. *Lysosomal Cysteine Proteinases*, 2nd ed.; Oxford University Press: Oxford, U.K., 1998; pp 52−54.

(26) Palmer, J. T.; Bryant, C.; Wang, D.-X.; Davis, D. E.; Setti, E. L.; Rydzewski, R. M.; Venkatraman, S.; Tian, Z.-Q.; Burrill, L. C.; Mendonca, R. V.; Springman, E.; McCarter, J.; Chung, T.; Cheung, H.; Janc, J. W.; McGrath, M.; Somoza, J. R.; Enriquez, P.; Yu, Z. W.; Strickley, R. M.; Liu, L.; Venuti, M. C.; Percival, M. D.; Falgueyret, J.-P.; Prasit, P.; Oballa, R.; Riendeau, D.; Young, R. N.;

Wesolowski, G.; Rodan, S. B.; Johnson, C.; Kimmel, D. B.; Rodan, G. Design and synthesis of tri-ring P_3 benzamide-containing aminonitriles as potent, selective, orally effective inhibitors of cathepsin K. *J. Med. Chem.* **2005**, *48*, 7520−7534.
(27) Prepared by dehydrating Cbz-Leu-Leu-Leu-NH_2 with trifluoroacetic anhydride.
(28) Wilk, S.; Figueiredo-Pereira, M. E. Synthetic inhibitors of the multicatalytic proteinase complex (proteasome). *Enzyme Protein* **1993**, *47*, 306−313.
(29) Bogyo, M.; Shin, S.; McMaster, J. S.; Ploegh, H. Substrate binding and sequence preference of the proteasome revealed by active-site-directed affinity probes. *Chem. Biol.* **1998**, *5*, 307−320.
(30) Robertson, J. G. Mechanistic basis of enzyme-targeted drugs. *Biochemistry* **2005**, *44*, 5561−5571.
(31) Binford, S. L.; Maldonado, F.; Brothers, M. A.; Weady, P. T.; Zalman, L. S.; Meador, J. W.; Matthews, D. A.; Patick, A. K. Conservation of amino acids in human rhinovirus 3C protease correlates with broad-spectrum antiviral activity of rupintrivir, a novel human rhinovirus 3C protease inhibitor. *Antimicrob. Agents Chemother.* **2005**, *49*, 619−626.
(32) Conversation with Professor Ralph Hirschmann.
(33) Perni, R. B.; Pitlik, J.; Britt, S. D.; Court, J. J.; Courtney, L. F.; Deininger, D. D.; Farmer, L. J.; Gates, C. A.; Harbeson, S. L.; Levin, R. B.; Lin, C.; Lin, K.; Moon, Y.-C.: Luong, Y.-P.; O′Malley, E. T.; Rao, B. G.; Thomson, J. A.; Tung, R. D.; Van Drie, J. H.; Wei, Y. Inhibitors of hepatitis C virus NS3-4A protease 2. Warhead SAR and optimization. *Bioorg. Med. Chem. Lett.* **2004**, *14*, 1441−1446.
(34) Nussbaum, A. K.; Dick, T. P.; Keilholz, W.; Schirle, M.; Stevanovic, S.; Dietz, K.; Heinemeyer, W.; Groll, M.; Wolf, D. H.; Huber, R.; Rammensee, H.-G.; Schild, H. Cleavage motifs of the yeast 20S proteasome β subunits deduced from digests of enolase I. *Proc. Natl. Acad. Sci. U.S.A.* **1998**, *95*, 12504−12509.
(35) Cyclohexyl esters, used in solid phase peptide synthesis because of their chemical robustness, typically require HF for deprotection.
(36) deFries, R.; Mitsuhashi, M. Quantification of mitogen induced human lymphocyte proliferation: comparison of alamarBlue assay to 3H-thymidine incorporation assay. *J. Clin. Lab. Anal.* **1995**, *9*, 89−95.
(37) Wacher, V. J.; Silverman, J. A.; Zhang, Y.; Benet, L. Z. Role of P-glycoprotein and cytochrome P450 3A in limiting oral absorption of peptides and peptidomimetics. *J. Pharm. Sci.* **1998**, *87*, 1322−1330.
(38) Falkiewicz, B.; Wisniowski, W.; Kolodziejczyk, A. S.; Wisnewski, K. Synthesis of new chiral peptide nucleic acids (PNA). *Nucleosides Nucleotides* **2001**, *20*, 1393−1397.
(39) Kuzmic, P.; Sideris, S.; Cregar, L. M.; Elrod, K. C.; Rice, K. D.; Janc, J. W. High-throughput screening of enzyme inhibitors: automatic determination of tight-binding inhibition constants. *Anal. Biochem.* **2000**, *281*, 62−67.
(40) Morrison, J. F. Kinetics of the reversible inhibition of enzyme-catalysed reactions by tight-binding inhibitors. *Biochim. Biophys. Acta* **1969**, *185*, 269−286.

JM058289O